Supporting Information:

Synthesis, Structure, Anion Binding and Sensing by Calix[4]pyrrole Isomers

Ryuhei Nishiyabu,[a] *Manuel A. Palacios,*[a] *Wim Dehaen,*[b] *and Pavel Anzenbacher, Jr.**[a]

[a] Department of Chemistry and Center for Photochemical Sciences, Bowling Green State University, Bowling Green, Ohio 43403, U.S.A.

[b] Department of Chemistry, Katholieke Universiteit Leuven, Celestijnenlaan 200F, 3001 Leuven, Belgium.

Contents:

General.

^{1}H and ^{13}C NMR spectra were recorded using a BRUKER 300 spectrometer (300 MHz for ^{1}H and 75 MHz for ^{13}C). EI DIP mass spectra were recorded using a Shimadzu QP5050A. Absorption spectra were recorded using a Hitachi U-3010. In absorption spectroscopic titrations and ^{1}H NMR titrations for anion binding studies, a receptor solution (solution **A**) was titrated by adding solutions of an anion that containing the same concentration of receptor with solution **A** for avoiding dilution of receptor concentration in the object to be examined. A titration curve obtained by plotting change in optical density at a wavelength (absorption spectroscopic titration) or chemical shift changes of a signal (^{1}H NMR titrations) was analyzed by a nonlinear least-squares method using a equation for 1:1 binding model.[1]

Synthesis.

All synthetic manipulations were performed under dry argon atmosphere using standard techniques. Octamethylcalix[4]pyrrole (**1**),[2] N-confused octamethylcalix[4]pyrrole (**2**),[3] and **TCE-1**[4] were prepared according to the procedures described in the literatures. Other materials were purchased and used as received.

Updated synthesis N-confused octamethylcalix[4]pyrrole (**2**) departs from the literature[3], however, some modifications have been made to maximize the yield of **2**. This updated procedure is as follows: To a solution of pyrrole (0.5 mol, 33.5 g) and acetone (0.5 mol, 29 g) in methanol (100 mL) methanesulfonic acid (1 mL) was added. The mixture was stirred at room temperature (exothermic reaction) for 3 hrs and all the solvent was removed *in vacuo*. The residue was taken up into dichloromethane (350 mL) and immediately before the column chromatography heptane (150 mL) was added. The column chromatography using silica gel and dichloromethane/heptane (70/30) yielded the normal calix[4]pyrrole (fraction 1, 34.5 g, 65%). After this isomer was removed, the chromatography was continued with pure dichloromethane to obtain the N-confused isomer (fraction 2, 8.2 g, 15%). Before evaporation of the dichloromethane, heptane (100 mL) was added to the fraction 2. The dichloromethane was removed from both fraction 1 and fraction 2, causing the products to crystallize from the residual heptane. After filtration, the products were washed with pentane (50 mL) and dried *in vacuo*.

N-confused calix[4]pyrrole **2**: 184-185° C, ^{1}H NMR (300MHz, $CDCl_3$, 25°C, TMS) δ = 1.45-1.56 (m, 24H, methyl), 5.52 (br, 1H, pyrrole β-H), 5.82 (m, 2H, pyrrole β-H), 5.98 (br, 2H, pyrrole β-H), 6.03 (br, 2H, pyrrole β-H), 6.40 (d, 1H, pyrrole α-H), 7.15 (br, 2H, pyrrole NH), 7.45 (br, 1H, pyrrole NH), 7.75 (br, 1H, pyrrole NH). ^{13}C NMR (75MHz, $CDCl_3$, 25°C, TMS) δ = 29.4, 29.8, 29.9, 30.7 (4x methyl), 35.0, 35.7, 35.8, 35.9 (4x meso C), 102.0, 102.2, 102.6, 103.2, 103.8, 104.4, 104.7 (7x pyrrole β-CH), 112.0 (pyrrole α-CH), 133.7 (pyrrole β-C), 138.0, 138.2, 138.7, 139.2, 139.3, 139.9, 141.5 (7x pyrrole α-C)

Azo-1: 4-Nitrobenzenediazonium tetrafluoroborate (1.4 g, 5.8 mmol) dissolved in THF (100 mL) was added to a solution of **1** (2.5 g, 5.8 mmol) and triethylamine (1 mL) in THF (30 mL) at 0 °C for 1 h. Then, removal of solvent from the reaction mixture obtained a dark red solid. The obtained solid dissolved in dichloromethane (500 mL) was washed with water (300 mL) and dried

over anhydrous Na_2SO_4. Purification by silica gel column chromatography (solvent: dichloromethane) afforded a yellow solid. Yield: 9% (470 mg). ^{1}H NMR (300 MHz, DMSO-d_6): δ = 1.52 (s, 6H, CH_3), 1.54 (s, 6H, CH_3), 1.58 (s, 6H, CH_3), 1.88 (s, 6H, CH_3), 5.68-5.72 (m, 4H, β-pyrrole CH), 5.87 (dd, *J* = 3.0, 3.0 Hz, 1H, β-pyrrole CH), 5.93 (dd, *J* = 3.0, 3.0 Hz, 1H, β-pyrrole CH), 6.25 (d, *J* = 2.7 Hz, 1H, β-pyrrole CH), 7.82 (d, *J* = 9.3 Hz, 2H, aryl CH), 8.34 (d, *J* = 9.3 Hz, 2H, aryl CH), 9.14 (br, 1H, pyrrole NH), 9.55 (br, 1H, pyrrole NH), 9.69 (br, 1H, pyrrole NH), 9.83 (br, 1H, pyrrole NH). ^{13}C NMR (75 MHz, $CDCl_3$): δ = 28.65 CH_3, 28.77 CH_3, 29.26 CH_3, 29.78 CH_3, 35.30 C, 35.38 C, 35.51 C, 37.88 C, 93.99 CH, 101.69 CH, 102.97 CH, 103.29 CH, 104.15 CH, 104.65 CH, 104.47 CH, 122.52 CH, 124.92 CH, 136.20 C, 136.71 C, 137.67 C, 138.59 C, 139.38 C, 139.74 C, 139.81 C, 140.36 C, 145.79 C, 147.34 C, 157.54 C. EI/MS (70 eV): z/m (%): 562 (48) $[M–CH_3]^+$, 577(100) $[M^+]$.

Azo-2: 4-Nitrobenzenediazonium tetrafluoroborate (54 mg, 0.23 mmol) dissolved in THF (10 mL) was added to a solution of **2** (100 mg, 0.23 mmol) in THF (30 mL) at 0 °C for 1 h. Then removal of solvent from the reaction mixture afforded a dark red solid. The obtained solid dissolved in dichloromethane (100 mL) was washed with water (100 mL) and dried over anhydrous Na_2SO_4. Purification by silica gel column chromatography (solvent: dichloromethane) afforded a red solid. Yield: 30% (40 mg). ^{1}H NMR (300 MHz, DMSO-d_6): δ = 1.53 (s, 12H, CH_3), 1.57 (s, 6H, CH_3), 1.74 (s, 6H, CH_3), 4.94 (br, 1H, β-pyrrole CH), 5.68 - 5.79 (m, 6H, β-pyrrole CH), 7.63 (d, *J* = 7.5 Hz, 2H, aryl H), 8.33 (d, *J* = 8.7 Hz, 2H, aryl H), 9.01 (br, 2H, NH), 9.29 (br, 1H, NH), 11.41 (br, 1H, NH); EI/MS (70 eV): z/m (%): 562 (54) $[M–CH_3]^+$, 577 (100) $[M^+]$; HRMS: 578.3243 $[M+H]^+$ calcd. for $C_{34}H_{40}N_7O_2$, found 578.3250.

TCE-2C: **2** (1.00 g, 2.33 mmol) and tetracyanoethylene (0.30 g, 2.33 mmol) were dissolved in THF (60 mL) and refluxed for 12h. Then removal of solvent afforded a brown solid. Purification by silica gel column chromatography (solvent: dichloromethane) obtained a purple solid. Yield: 36% (450 mg). ^{1}H NMR (300 MHz, $CDCl_3$): δ = 1.578 (s, 6H, CH_3), 1.582 (s, 6H, CH_3), 1.68 (s, 6H, CH_3), 1.74 (s, 6H, CH_3), 4.36 (s, 1H, β-pyrrole CH), 5.85 (dd, *J* = 3.0, 3.0 Hz, 1H, β-pyrrole CH), 5.89 (dd, *J* = 3.0, 3.0 Hz, 1H, β-pyrrole CH), 5.95-6.00 (m, 4H, β-pyrrole CH), 7.16 (br, 1H, pyrrole NH), 7.38 (br, 2H, pyrrole NH), 9.42 (s, 1H, imine NH). (300 MHz, DMSO-d_6): δ = 1.50 (s, 6H, CH_3), 1.52 (s, 6H, CH_3), 1.61 (s, 6H, CH_3), 1.68 (s, 6H, CH_3), 4.77 (s, 1H, β-pyrrole CH),

5.67 (dd, *J* = 3.0, 3.0 Hz, 1H, β-pyrrole CH), 5.73-5.76 (m, 4H, β-pyrrole CH), 5.81 (dd, *J* = 3.0, 3.0 Hz, 1H, β-pyrrole CH), 8.53 (br, 1H, pyrrole NH), 9.19 (br, 1H, pyrrole NH), 9.45 (br, 1H, pyrrole NH), 11.16 (s, 1H, imine NH). ^{13}C NMR (75 MHz, $CDCl_3$): δ = 20.72 CH_3, 28.86 CH_3, 30.17 CH_3, 35.27 C, 35.29 C, 36.50 C, 37.39 C, 102.02 CH, 102.37 CH, 103.50 CH, 103.72 CH, 104.65 CH, 104.99 CH, 106.85 C, 111.05 C, 111.66 C, 118.14 CH, 121.42 C, 127.95 C, 136.79 C, 137.29 C, 138.41 C, 138.54 C, 139.02 C, 139.35 C, 144.65 C, 152.73 C, 154.78 C. EI/MS (70 eV): z/m (%): 514 (100) $[M–CH_3]^+$, 529 (67) $[M^+]$.

X-ray Structural Analysis. The data were collected on a Nonius Kappa CCD diffractometer using a graphite monochromator with Mo Kα radiation (λ = 0.71073 Å). The data were collected at 153 K using an Oxford Cryostream low temperature device. Data reduction were performed using DENZO-SMN.[5] The structures were solved by direct methods using SIR97[6] and refined by full-matrix least-squares on F^2 with anisotropic displacement parameters for the non-H atoms using SHELXL-97.[7] The hydrogen atoms on carbon were calculated in ideal positions with isotropic displacement parameters set to 1.2U_{eq} of the attached atom (1.5U_{eq} for methyl hydrogen atoms). Neutral atom scattering factors and values used to calculate the linear absorption coefficient are from the *International Tables for X-ray Crystallography* (1992).[8]

2: $2[C_{28}H_{36}N_4 – 2(C_2H_6SO)]$; crystals grew as yellow prisms by slow evaporation from DMSO. The data crystal was cut from a larger crystal and had approximate dimensions; 0.35 x 0.20 x 0.20 mm: monoclinic, space group P21, a = 10.4478(2) Å, b = 32.2490(6) Å, c = 10.6105(2) Å, α = 90°, β = 112.259(1)°, γ = 90°, V = 3308.60(11) Å^3, Z = 4, ρ_{calcd} = 1.174 mg m^{-3}, μ = 0.194 mm^{-1}, F(000) = 1264. A total of 376 frames of data were collected using ω-scans with a scan range of 0.6° and a counting time of 138 seconds per frame. A total of 12474 reflections were measured. The structure was refined on F^2 to 0.184, with *R(F)* equal to 0.0709 and a goodness of fit S = 1.00.

Azo-1: $(C_{34}H_{39}N_7O_2) – 2C_3H_7NO$; crystals grew as orange lathes by slow evaporation from *N*,*N*-dimethylformamide. The data crystal was cut from a cluster of crystals and had approximate dimensions; 0.25 x 0.21 x 0.13 mm: monoclinic, space group C2/c, a = 39.1329(7) Å, b = 9.8179(2) Å, c = 21.5984(5) Å, α = 90°, β = 102.7110(10)°, γ = 90°, V = 8094.8(3) Å^3, Z = 8, ρ_{calcd} = 1.188 mg m^{-3}, μ = 0.079 mm^{-1}, F(000) = 3104. A total of 407 frames of data were collected

using ω-scans with a scan range of 1° and a counting time of 151 seconds per frame. A total of 13634 reflections were measured, 7108 unique (R_{int} = 0.1187). The structure was refined on F^2 to 0.107, with *R(F)* equal to 0.0546 and a goodness of fit *S* = 1.052.

Azo-2: $C_{34}H_{39}N_7O_2$ – CH_2Cl_2; crystals grew as orange plates by slow evaporation from dichloromethane and diethyl ether. The data crystal was cut from a large plate and had approximate dimensions; 0.26 x 0.24 x 0.14 mm: triclinic, space group P-1, a = 9.9850(2) Å, b = 11.9288(2) Å, c = 15.2616(3) Å, α = 81.2270(10)°, β = 73.4380(10)°, γ = 73.8120(10)°, *V* = 1668.02(5) Å^3, *Z* = 2, ρ_{calcd} = 1.319 mg m^{-3}, μ = 0.238 mm^{-1}, *F*(000) = 700. A total of 549 frames of data were collected using ω-scans with a scan range of 1° and a counting time of 106 seconds per frame. A total of 12862 reflections were measured, 7569 unique (R_{int} = 0.0349). The structure was refined on F^2 to 0.119, with *R(F)* equal to 0.0486 and a goodness of fit *S* = 1.03.

TCE-1: $(C_{33}H_{35}N_7)_2$ – C_4H_8O; Crystals grew as orange lathes by slow evaporation from diethyl ether. The data crystal was a long lathe that had approximate dimensions; 0.46 x 0.21 x 0.06 mm: triclinic, space group P-1, a = 10.4865(3) Å, b = 16.8082(5) Å, c = 19.0923(6) Å, α = 91.479(2)°, β = 102.499(2)°, γ = 104.159(2)°, *V* = 3174.58(16) Å^3, *Z* = 2, ρ_{calcd} = 1.186 mg m^{-3}, μ = 0.073 mm^{-1}, *F*(000) = 1212. A total of 449 frames of data were collected using ω-scans with a scan range of 1° and a counting time of 153 seconds per frame. A total of 18976 reflections were measured, 11148 unique (R_{int} = 0.0997). The structure was refined on F^2 to 0.156, with *R(F)* equal to 0.0717 and a goodness of fit *S* = 1.00.

Figure S1. View of **2** showing the atom labeling scheme. Displacement ellipsoids are scaled to the 30% probability level. The methyl hydrogen atoms have been removed for clarity.

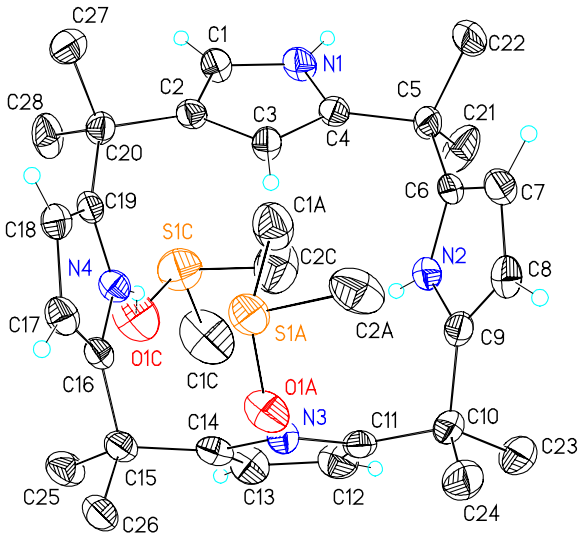

Figure S2. View of **2'** showing the atom labeling scheme. Displacement ellipsoids are scaled to the 30% probability level. The methyl hydrogen atoms have been removed for clarity.

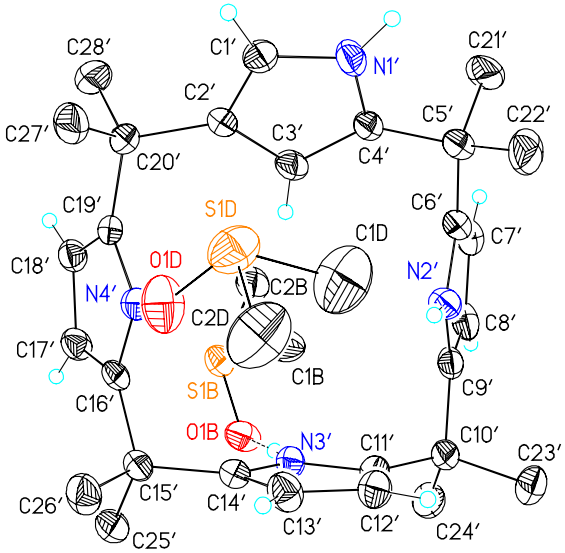

Figure S3. Unit cell packing diagram for **2**. The view is approximately down the **a** axis. The calixpyrroles pack in columns parallel to the **c** axis and bridged by the ordered molecules of DMSO. Macrocycles **2** are shown in ball-and-stick form, while macrocyles **2'** are in wireframe form. Dashed lines are indicative of H-bonding interactions.

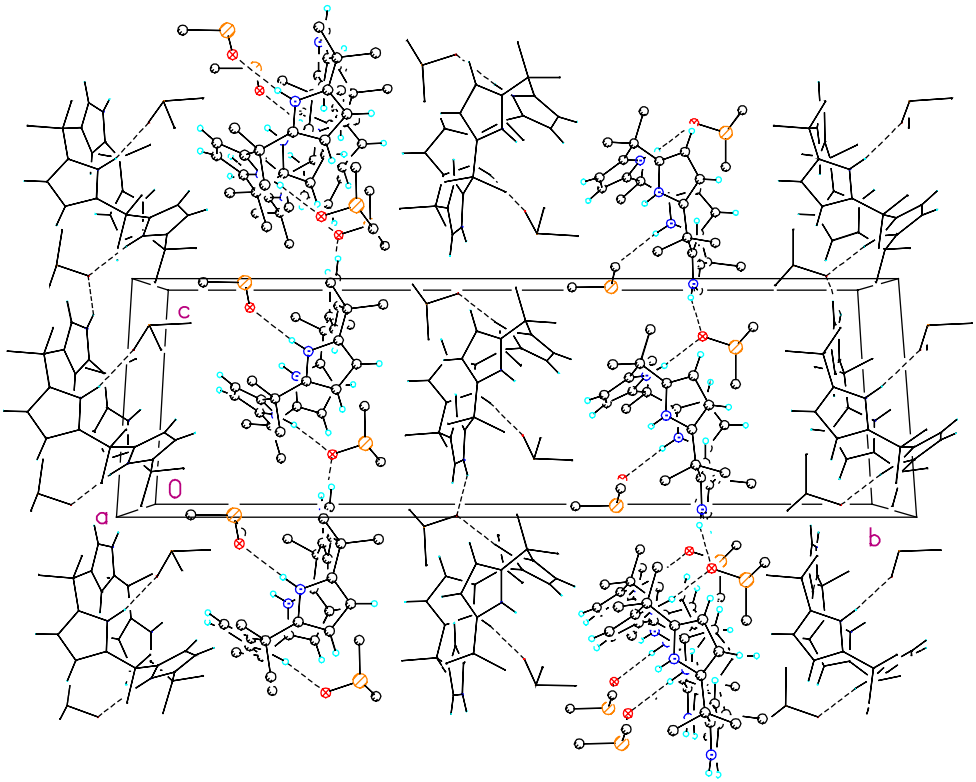

Figure S4. View of **TCE-1** showing the atom labeling scheme. Displacement ellipsoids are scaled to the 50% probability level.

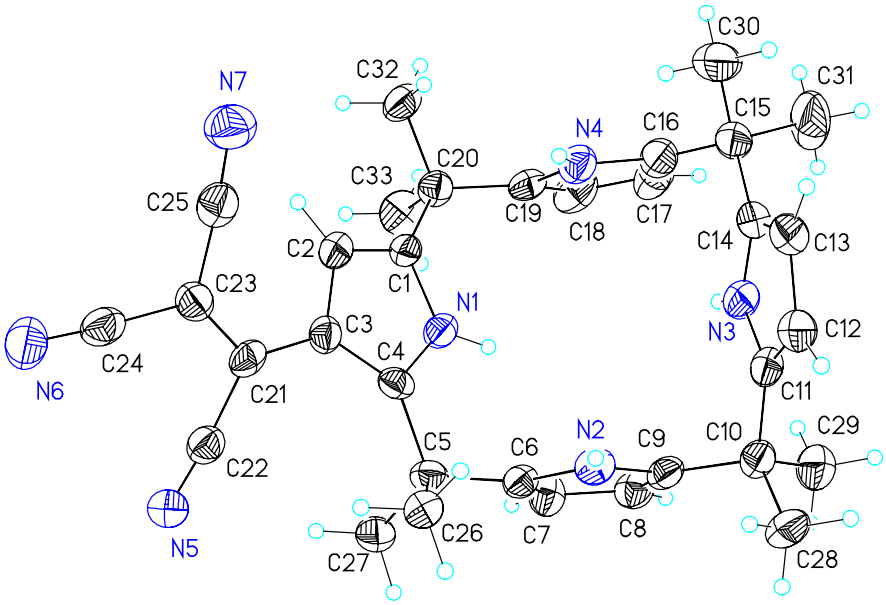

Figure S5. View of **TCE-1'** showing the atom labeling scheme. Displacement ellipsoids are scaled to the 50% probability level.

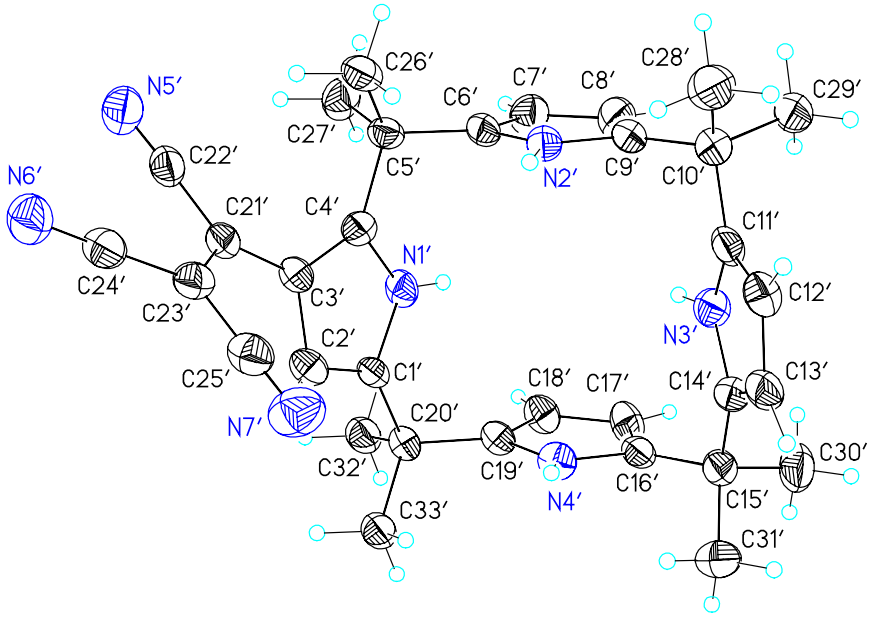

Figure S6. View showing the fit by least-squares of selected atoms of **TCE-1** (dashed lines) onto the equivalent atoms of **TCE-1'** (solid lines). Atoms of **TCE-1'** used in the fit are labeled.

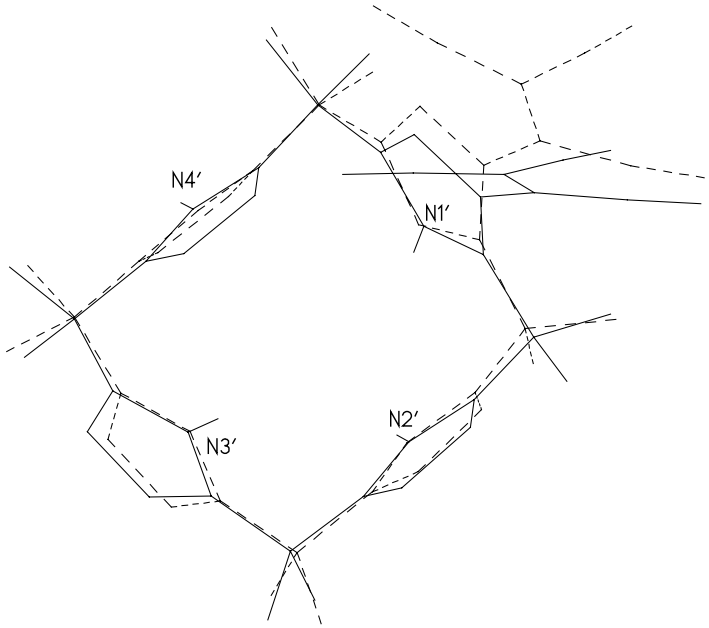

Figure S7. Unit cell packing diagram for **TCE-1**. The view is approximately down the **a** axis. Molecules **TCE-1** are shown in ball-and-stick form, while molecules **TCE-1'** are in wireframe display. Dashed lines are indicative of H-bonding interactions.

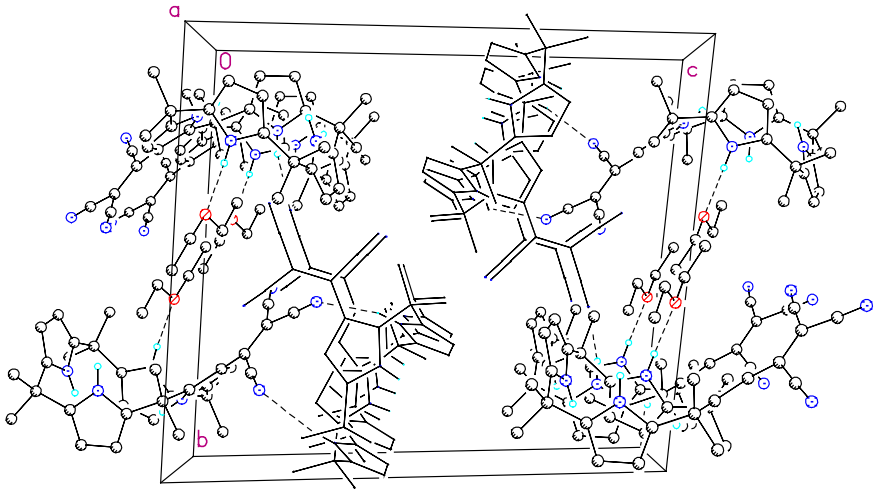

Figure S8. Unit cell packing diagram for **TCE-2C**. The view is approximately down the **a** axis. Molecules **TCE-2C** are shown in ball-and-stick form, while molecules **TCE-2C'** are in wireframe display. Dashed lines are indicative of H-bonding interactions.

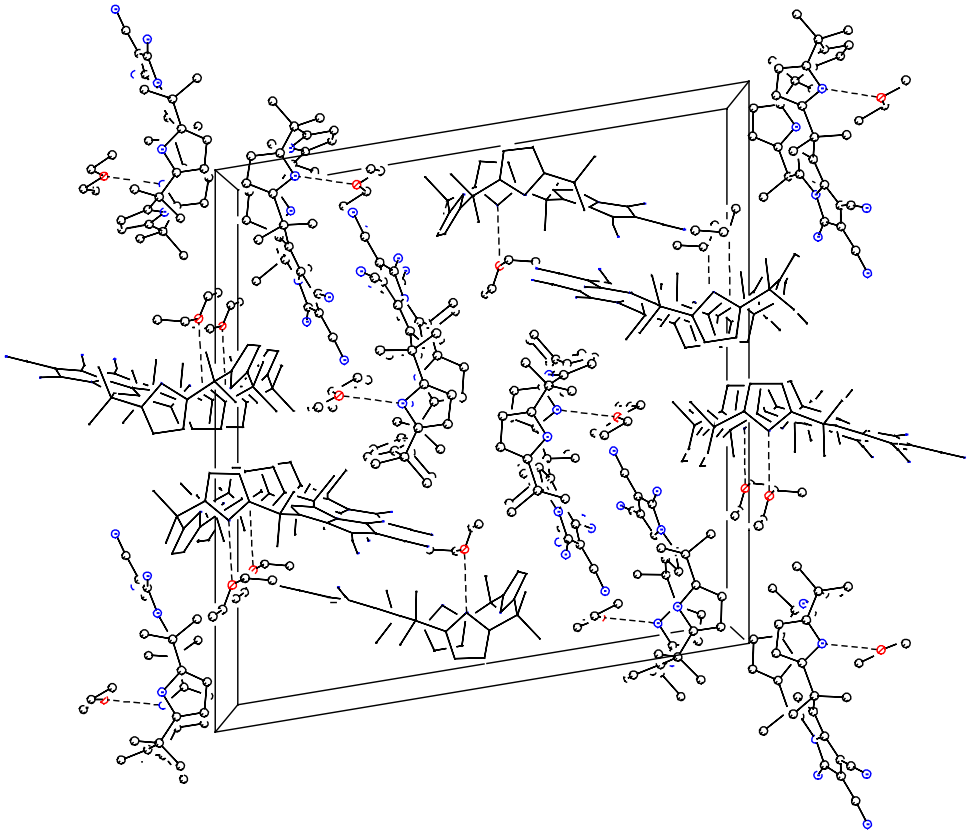

Figure S9. View of **Azo-1** showing the atom labeling scheme. Displacement ellipsoids are scaled to the 50% probability level.

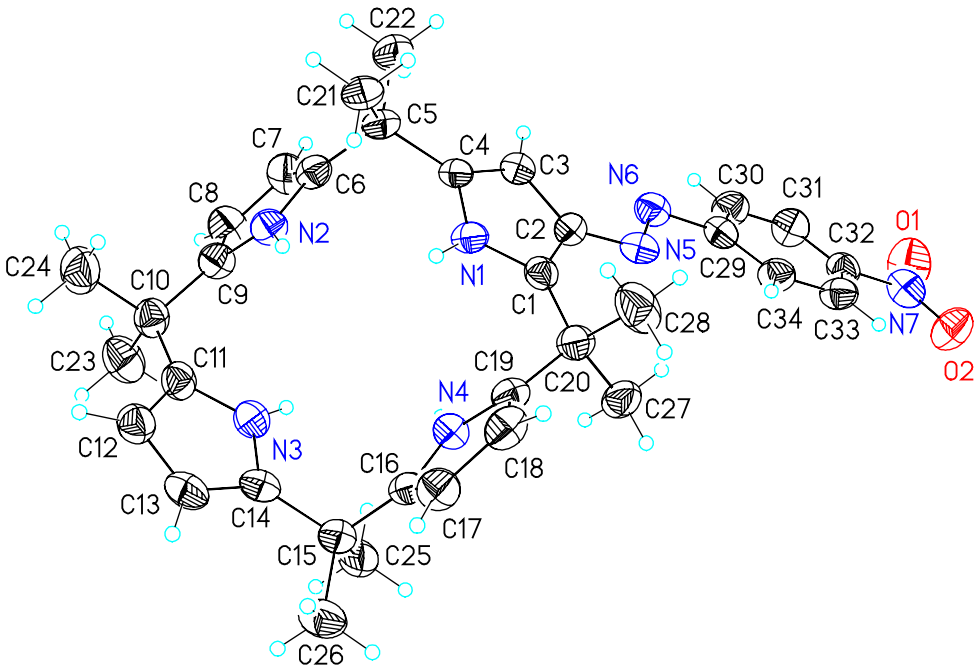

Figure S10. Unit cell packing diagram for **Azo-1**. The view is approximately down the **b** axis. Dashed lines are indicative of H-bonding interactions between the calixpyrrole and the solvent. The geometry of these interactions are: N1-H1N···O1b, N···O 2.916(3)Å, H···O 2.03(3)Å, N-H···O 164(3)°; N2-H2N···O1b, N···O 2.890(3)Å, H···O 1.93(3)Å, N-H···O 166(3)°; N3-H3N···O1a, N···O 2.991(4)Å, H···O 2.18(2)Å, N-H···O 171(3)°; N4-H4N···O1a, N···O 2.914(3)Å, H···O 2.01(3)Å, N-H···O 161(3)°.

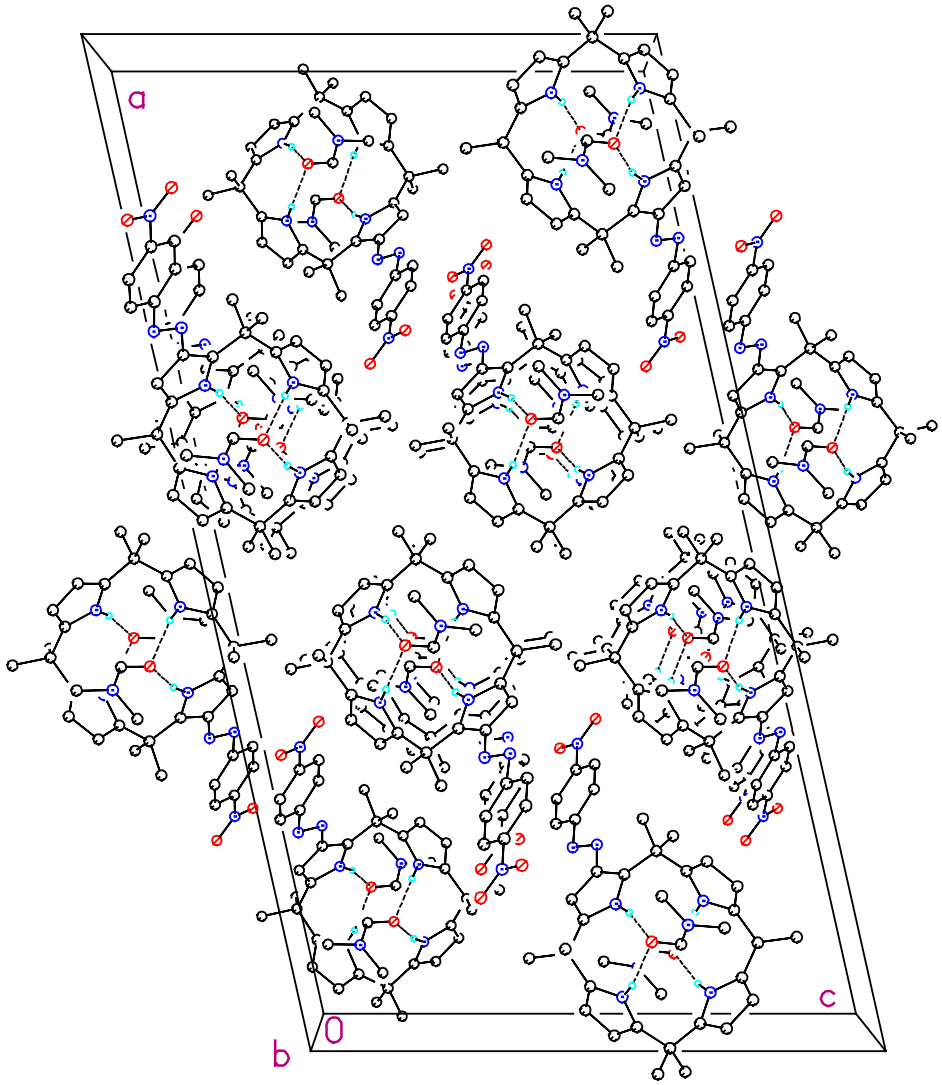

Figure 11. View of **Azo-2** showing the atom labeling scheme. Displacement ellipsoids are scaled to the 50% probability level. The methyl hydrogen atoms have been removed for clarity.

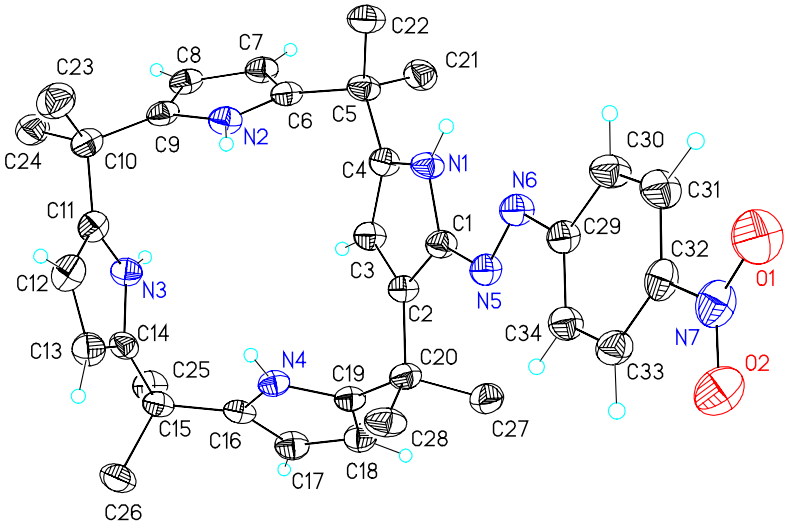

Figure S12. View illustrating the H-bound dimer formed in **Azo-2**. Displacement ellipsoids are scaled to the 50% probability level. Most hydrogen atoms have been removed for clarity. The dimer lies around a crystallographic at ½, ½, 0. Dashed lines are indicative of H-bonding interactions. The geometry of these interactions are: N2-H2N···O2 (related by 1-x, 1-y, -z); N···O 3.083(2)Å, H···O 2.21(2)Å, N-H···O 162(2)°; N4-H4N···O1 (related by 1-x, 1-y, -z); N···O 3.281(2)Å, H···O 2.45(2)Å, N-H···O 157(2)°.

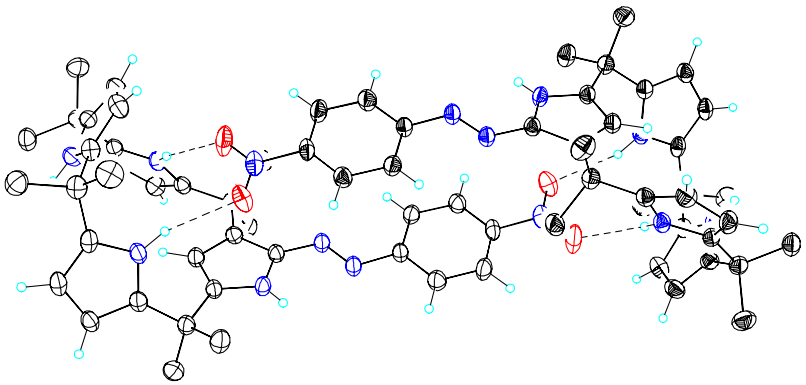

Figure S13. Unit cell packing diagram for **Azo-2**. The view is approximately down the **a** axis.

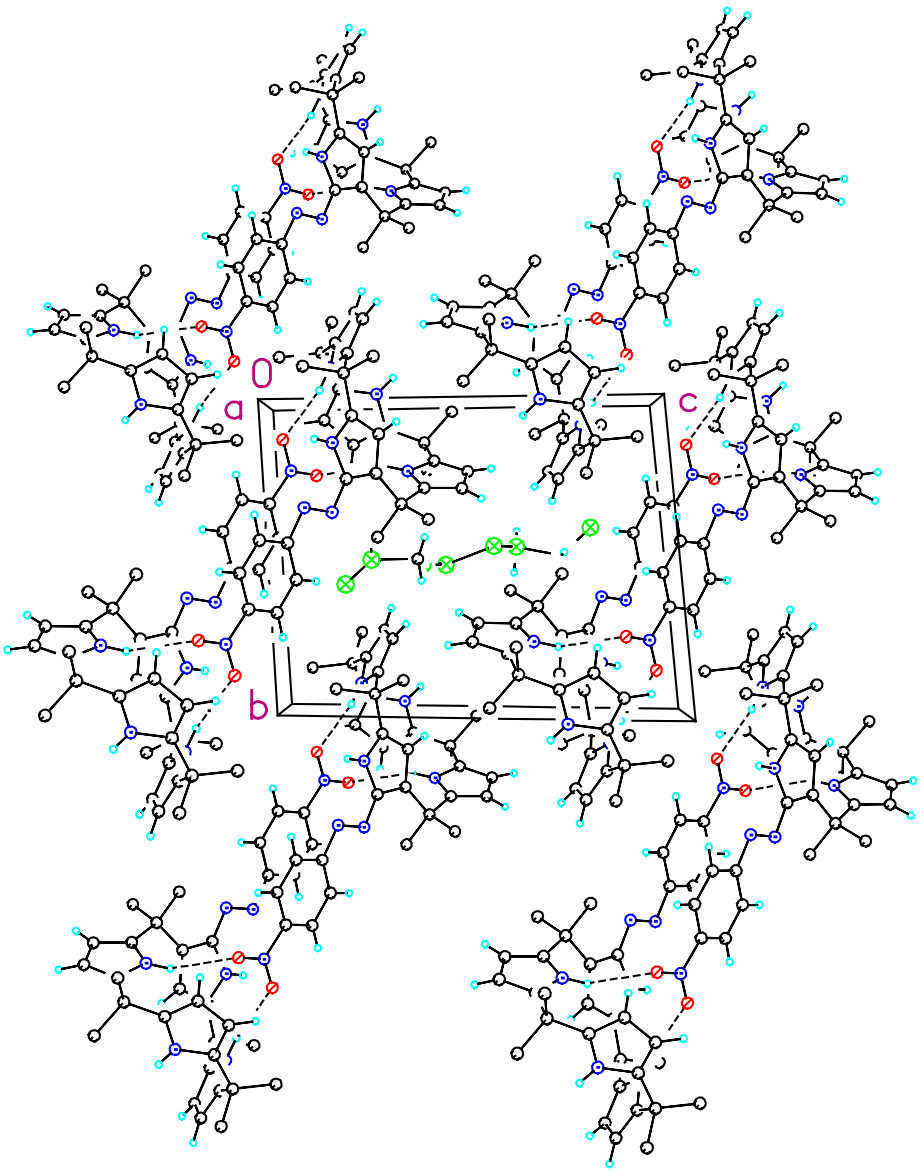

Figure S14. View illustrating the H-bonding interaction between the DMSO solvate molecules and **Azo-2**. Displacement ellipsoids are scaled to the 50% probability level. Most hydrogen atoms have been removed for clarity. Dashed lines are indicative of H-bonding interactions. The geometry of these interactions are: N1-H1N···O1B, N···O 2.825(4)Å, H···O 1.99(4)Å, N-H···O 161(3)°; N4-H4N···O1A, N···O 2.892(4)Å, H···O 2.08(3)Å, N-H···O 174(3)°.

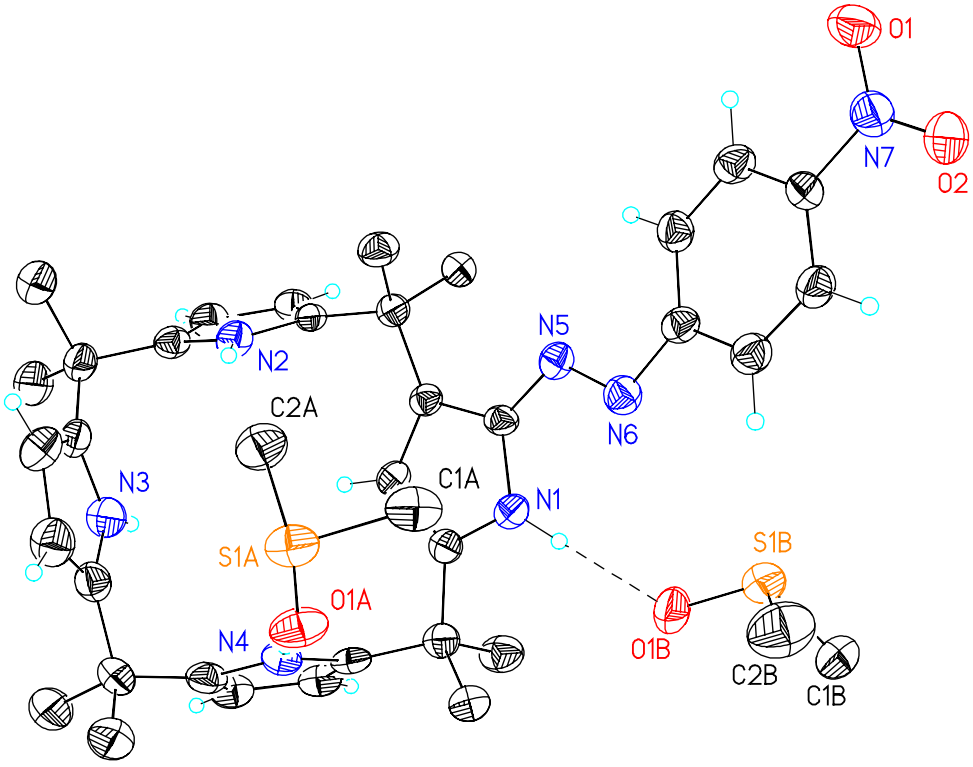

Figure S15. Unit cell packing diagram for **Azo-2**. The view is approximately down the **b** axis.

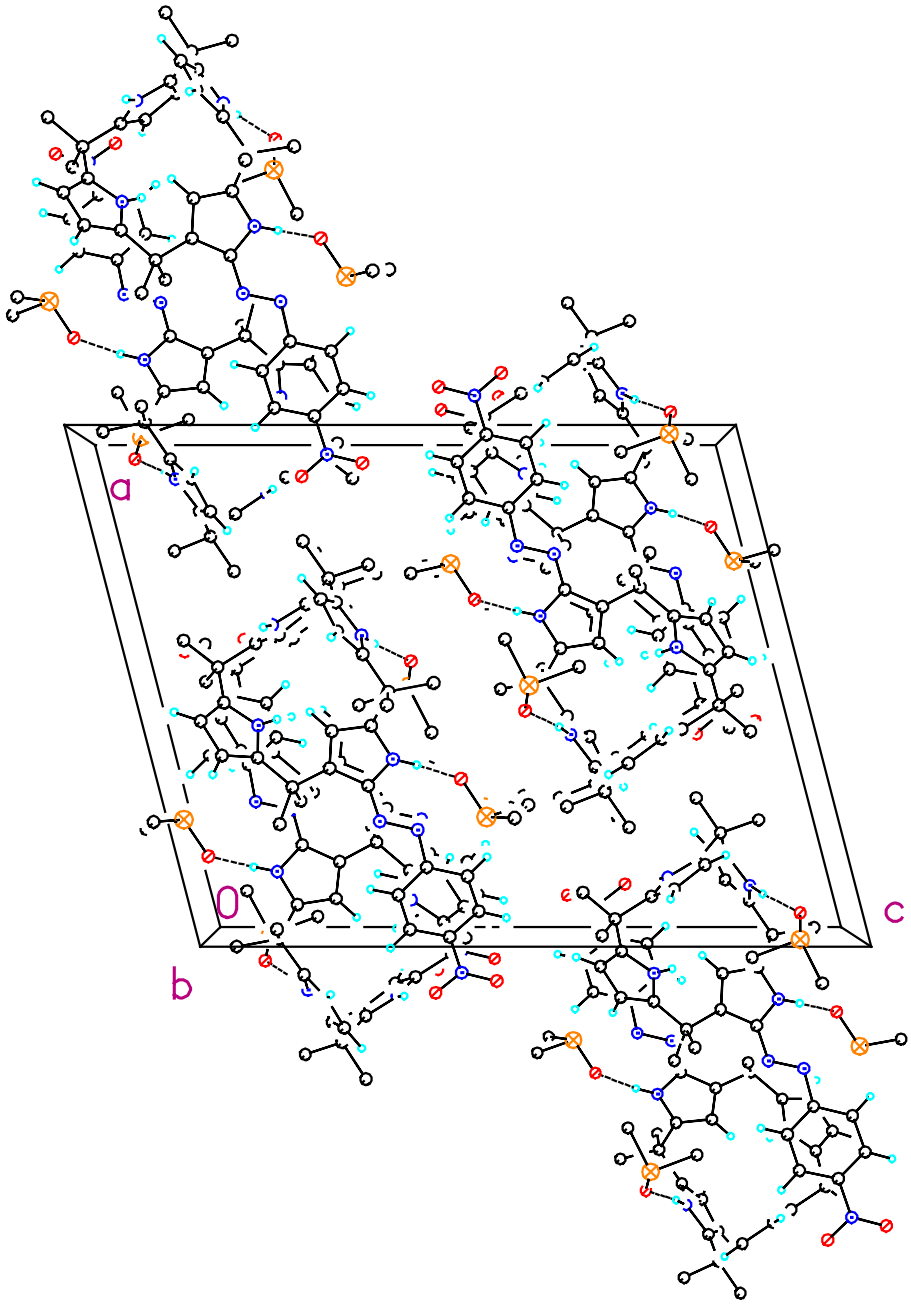

Absorption spectroscopic titration study.

Figure S16. Absorption spectroscopic titrations of **TCE-2C** ($5x10^{-5}$ M) with anions.

TCE-2C / F^-

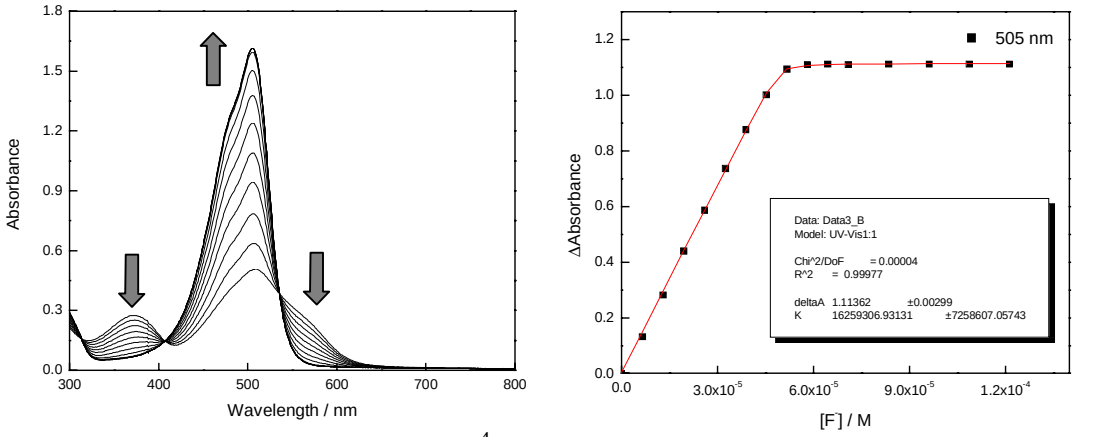

TCE-2C / Cl^- ([**TCE-2C**] = 1.0 x 10^{-4} M)

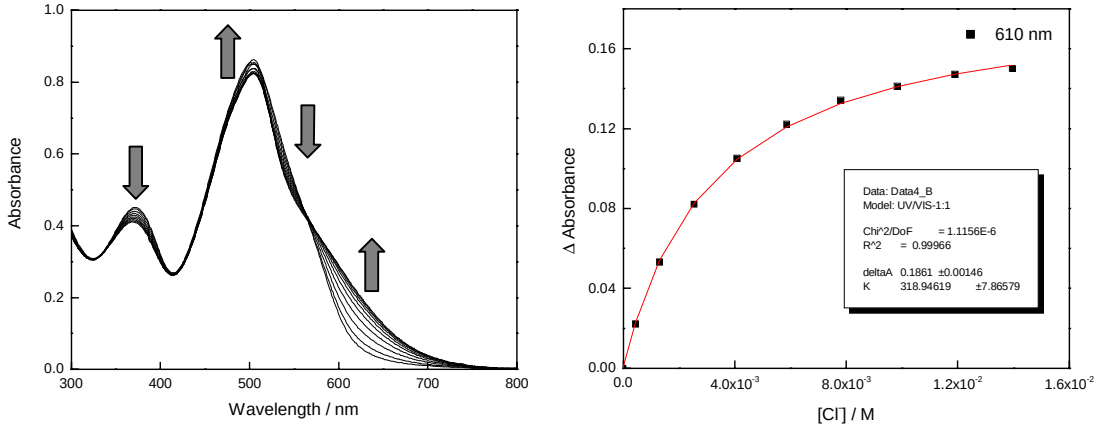

TCE-2C / AcO^-

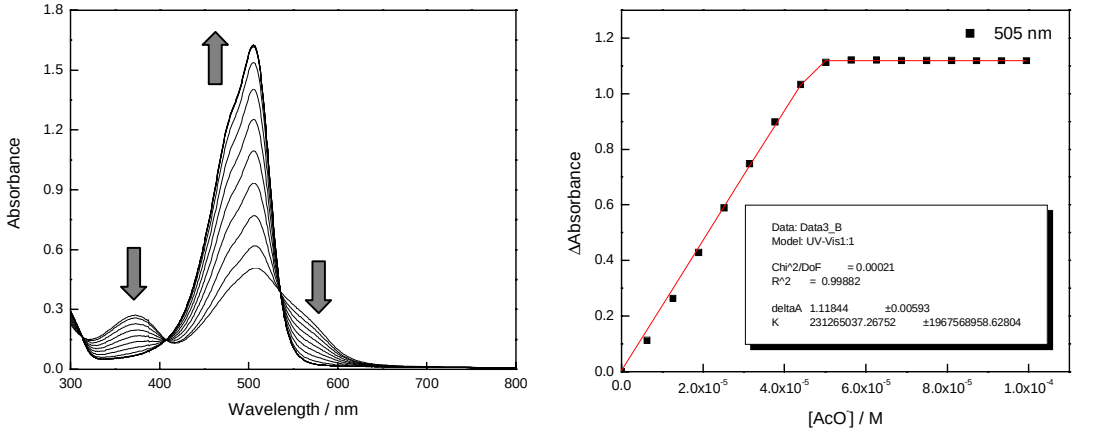

TCE-2C / $H_2PO_4^-$

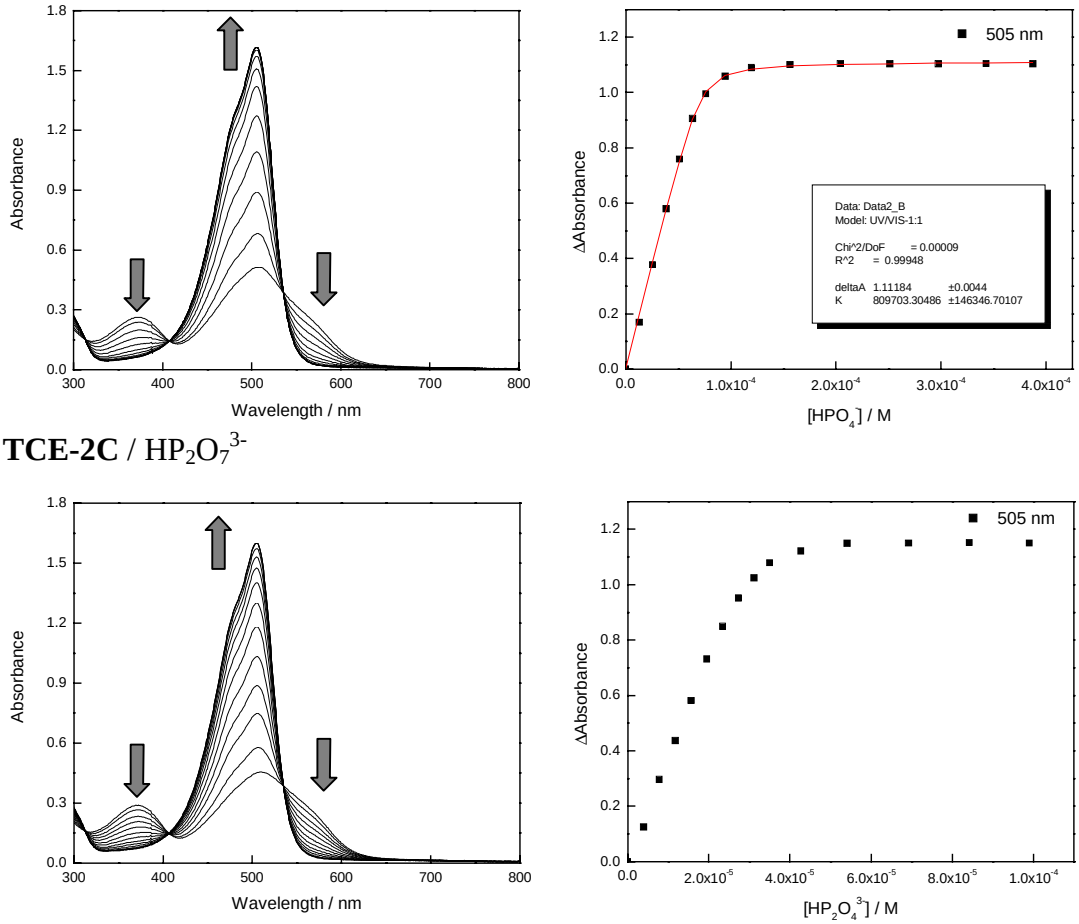

TCE-2C / $HP_2O_7^{3-}$

Figure S17. Color changes of **TCE-2C** ($5x10^{-5}$ M) in DMSO upon the addition of anions (10 equiv.).

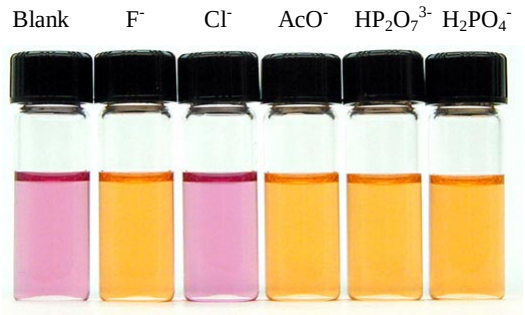

Figure S18. Absorption spectroscopic titrations of **Azo-1** ($5x10^{-5}$ M) with anions in DMSO.

Azo-1 / F^-

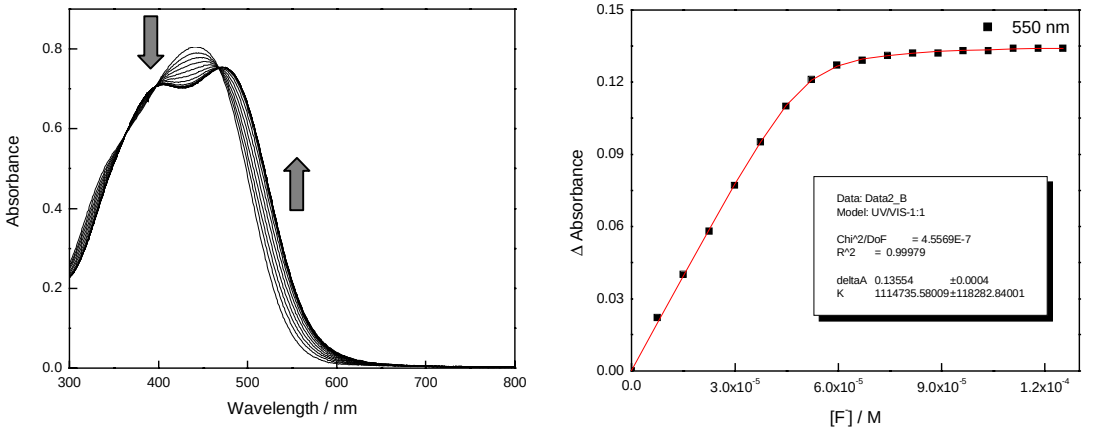

Azo-1 / Cl^-

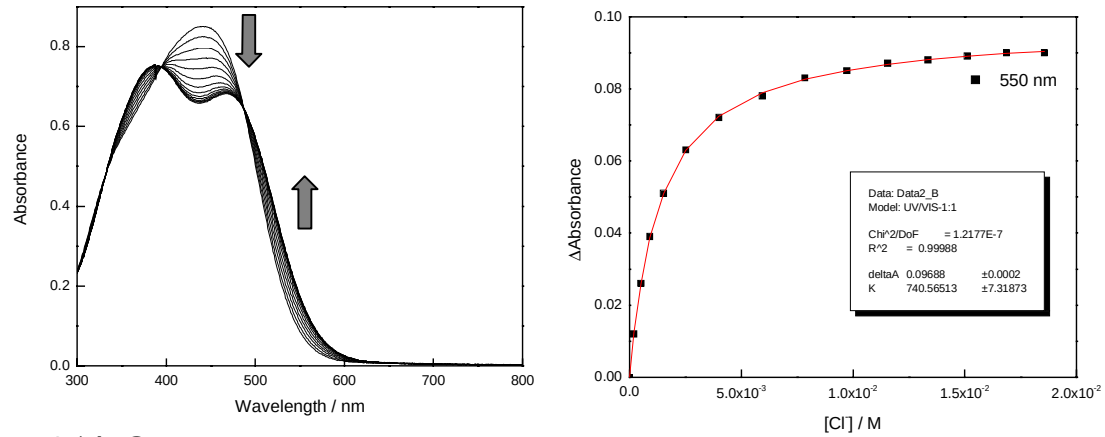

Azo-1 / AcO^-

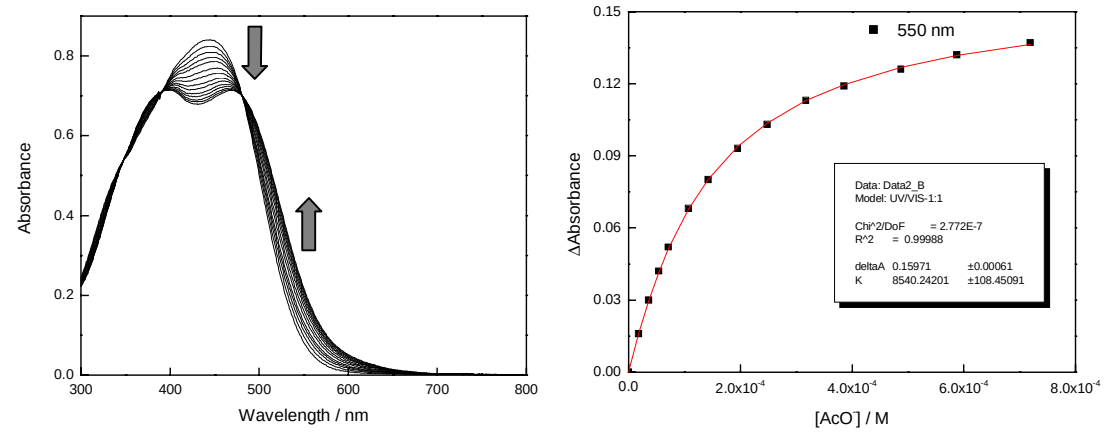

Azo-1 / $H_2PO_4^-$

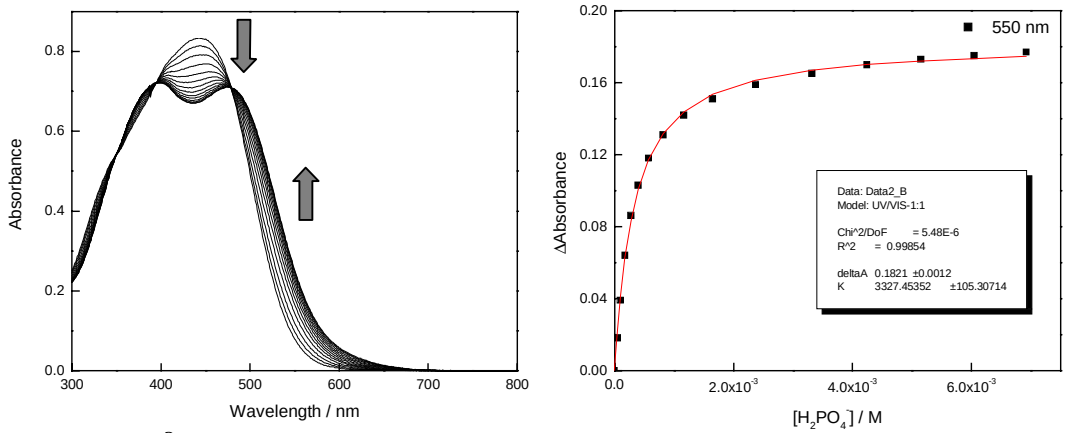

Azo-1 / $HP_2O_7^{3-}$

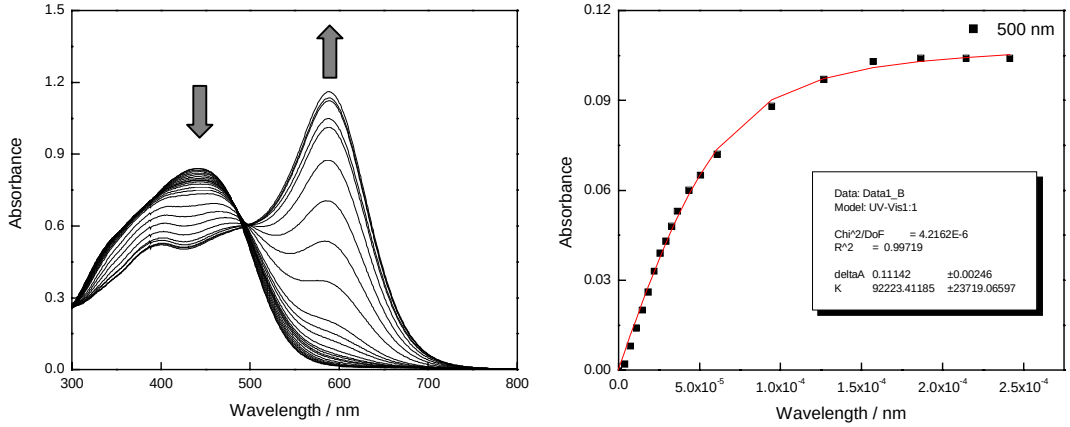

Figure S19. Color changes of **Azo-1** ($5x10^{-5}$ M) in DMSO upon the addition of anions (10 equiv.).

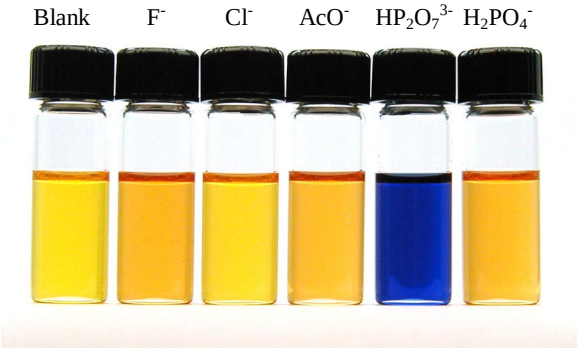

Figure S20. UV-vis titrations of sensor **Azo-2** (2.5×10^{-5} M) with anions in DMSO.

Azo-2 / F^-

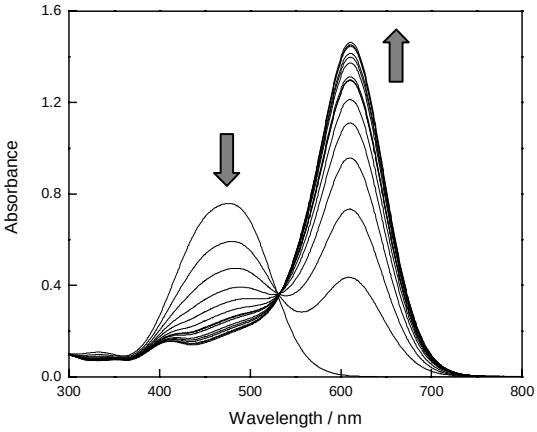

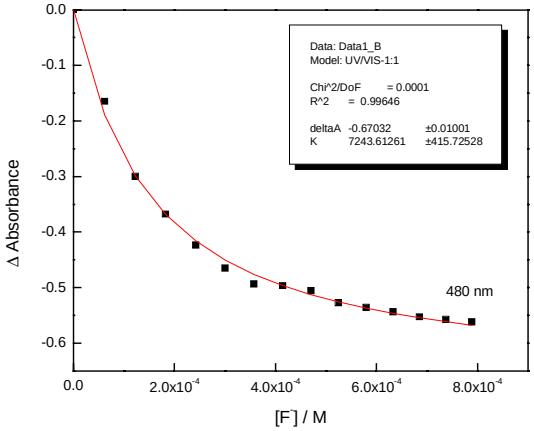

Azo-2 / Cl^-

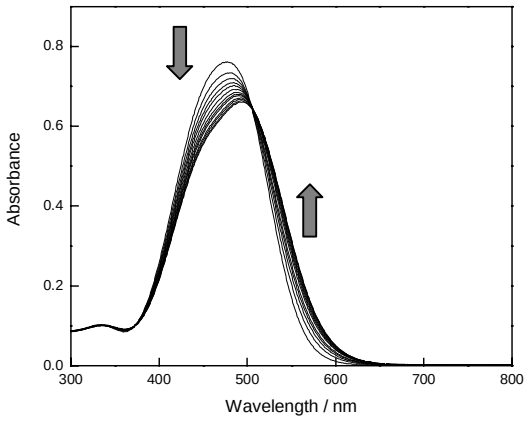

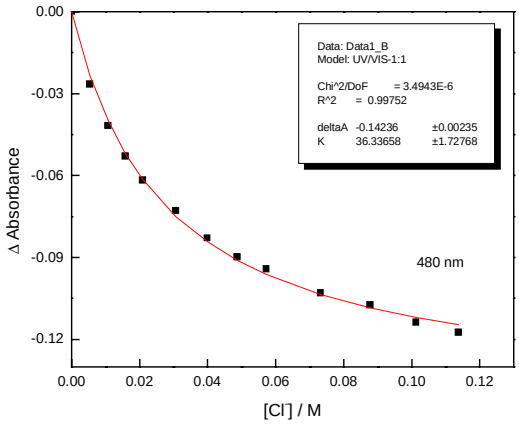

Azo-2 / AcO^-

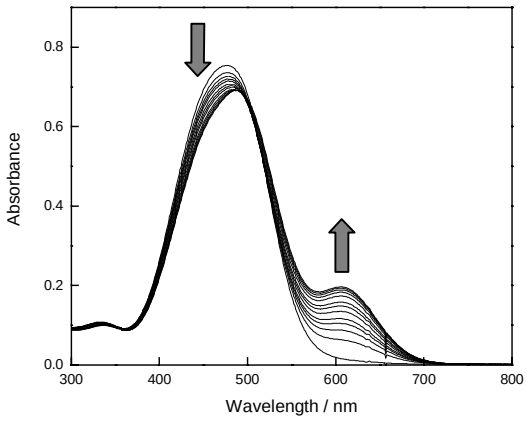

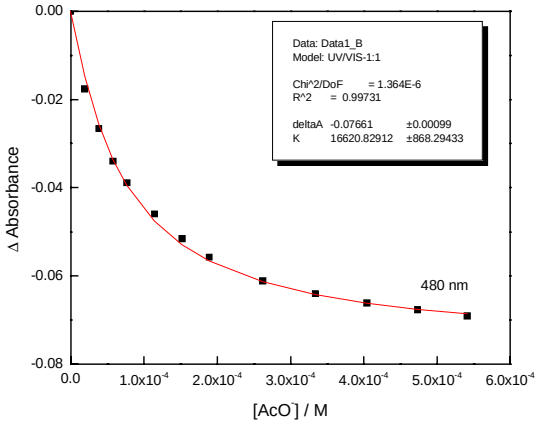

Azo-2 / $H_2PO_4^-$

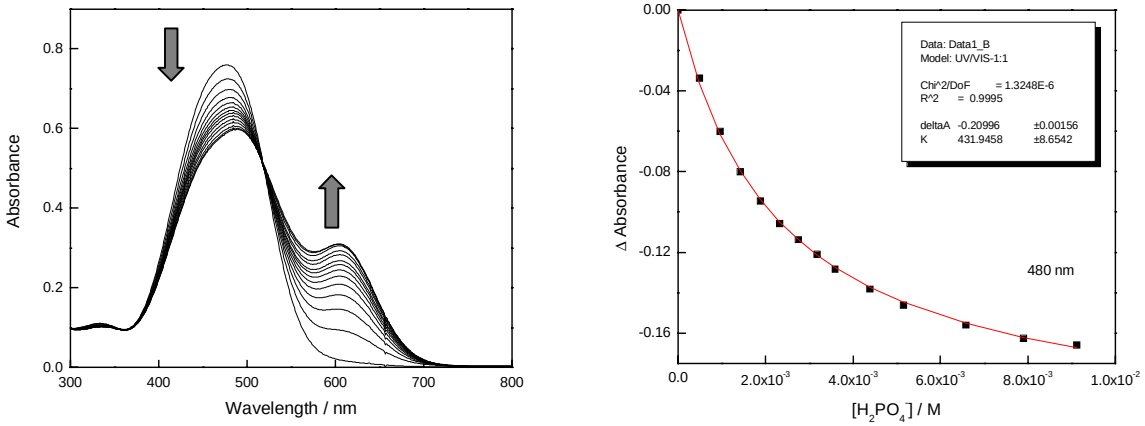

Azo-2 / $HP_2O_7^{3-}$

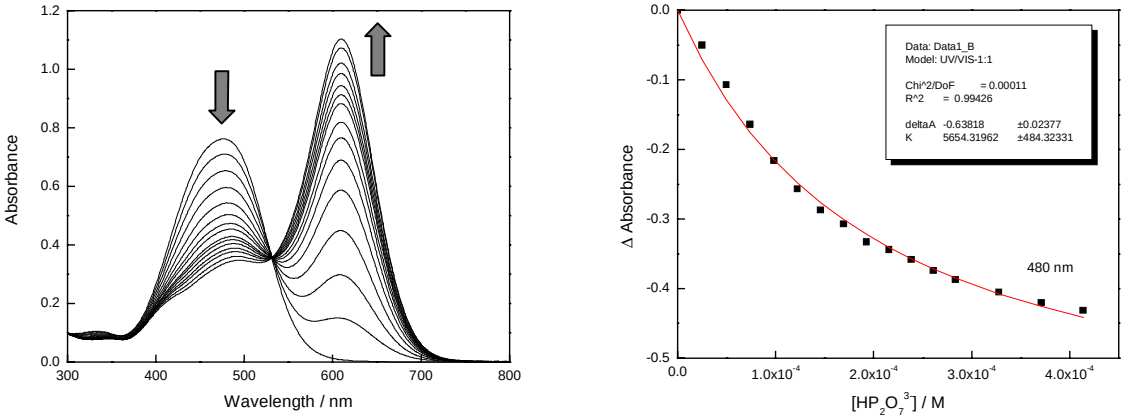

Figure S21. Color changes of **Azo-2** ($5x10^{-5}$ M) in DMSO upon the addition of anions (10 equiv.).

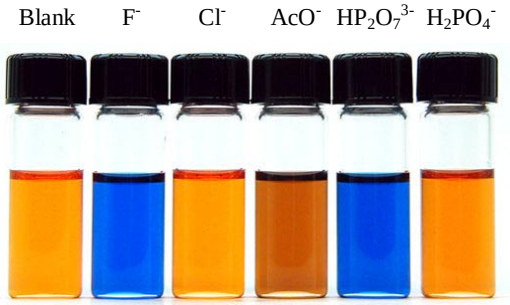

^{1}H NMR titration studies.

Figure S22. ^{1}H NMR titration of **1** (1.0×10^{-2} M) with Cl^- in DMSO-d_6.

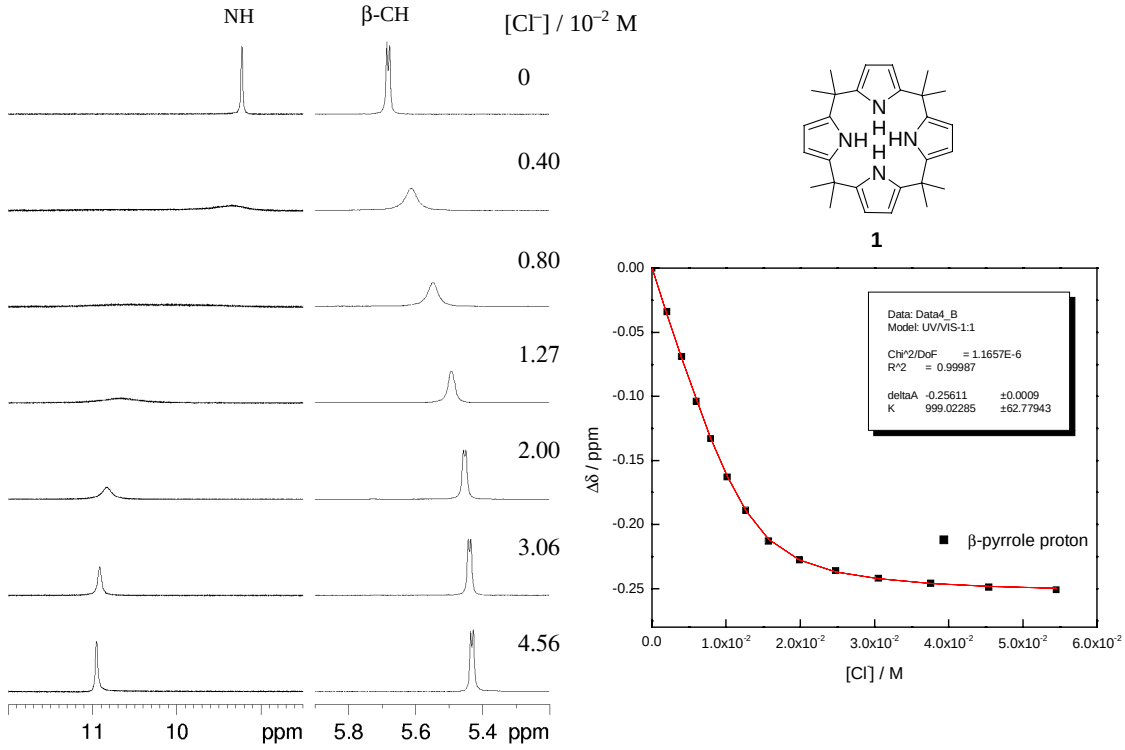

Figure S23. ^{1}H NMR titration of **2** (1.0×10^{-2} M) with Cl^- in DMSO-d_6. The inverted pyrrole ^{1}H resonances in **2** are labeled as follows: pyrrole NH_i ●, α-CH_i ●, and β-CH_i ●.

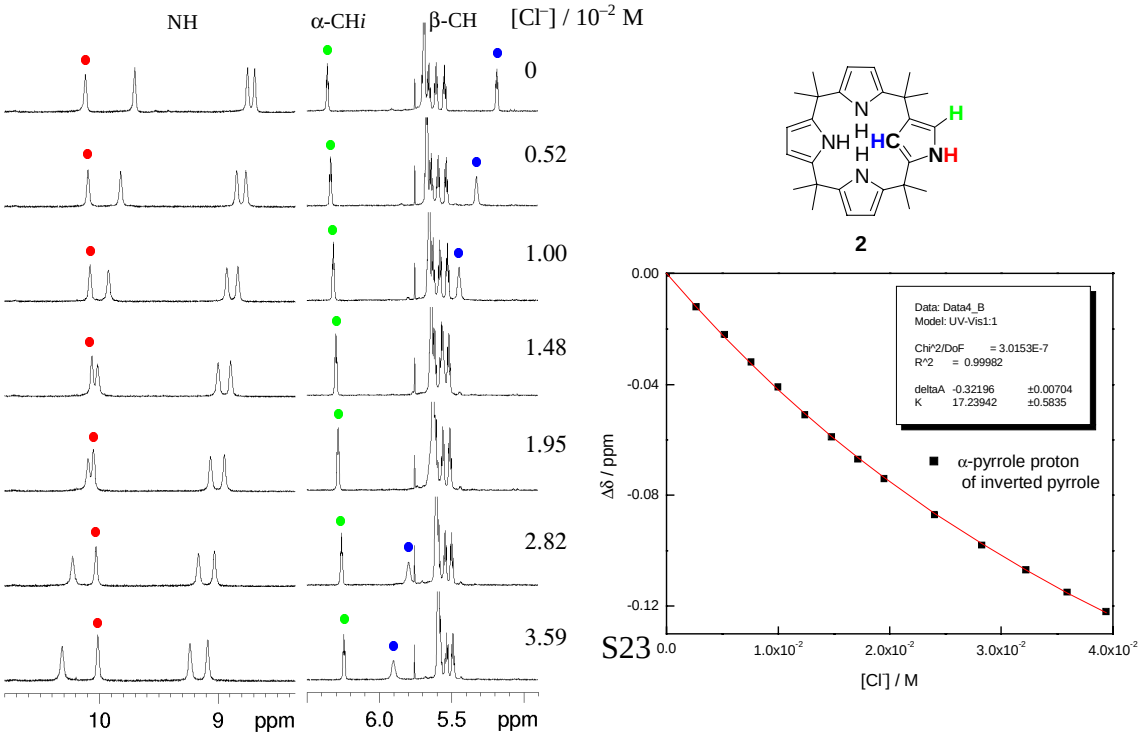

Figure S24. ^{1}H-NMR titration of **TCE-1** (1.0×10^{-2} M) with Cl^- in DMSO-d_6.

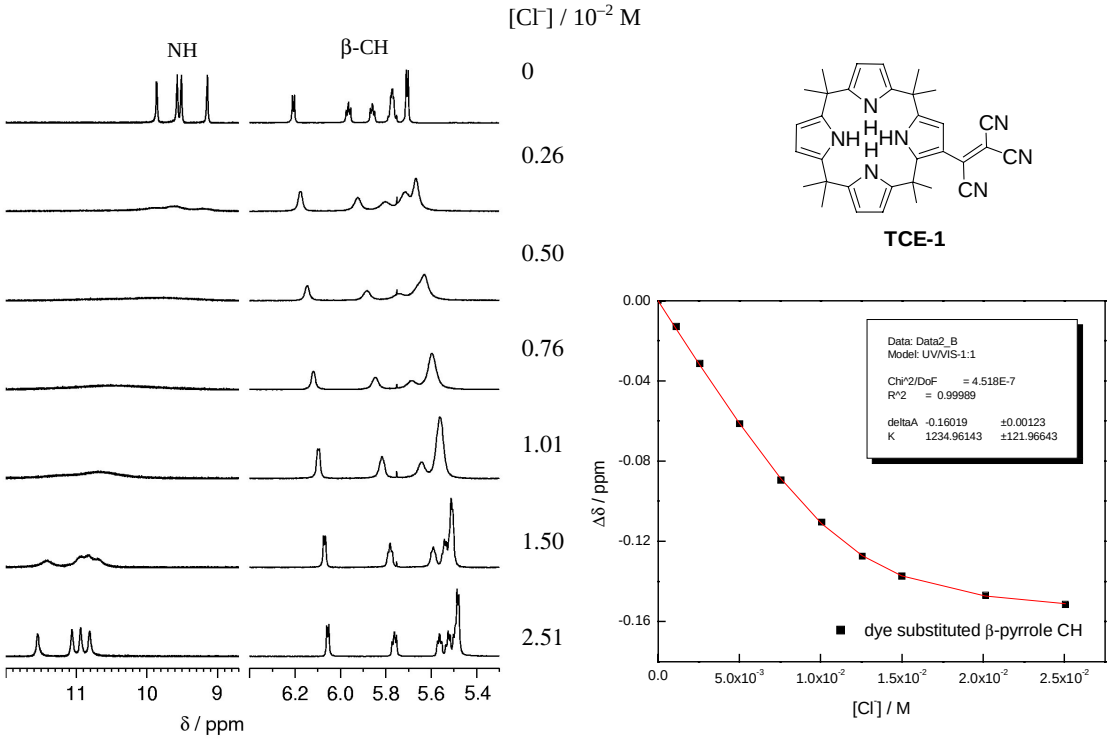

Figure S25. ^{1}H NMR titration of **TCE-2C** (1.0×10^{-2} M) with Cl^- in DMSO-d_6. The inverted pyrrole ^{1}H resonances in **TCE-2C** are labeled as follows: imine NH_i ● and pyrrole β-CH_i ●.

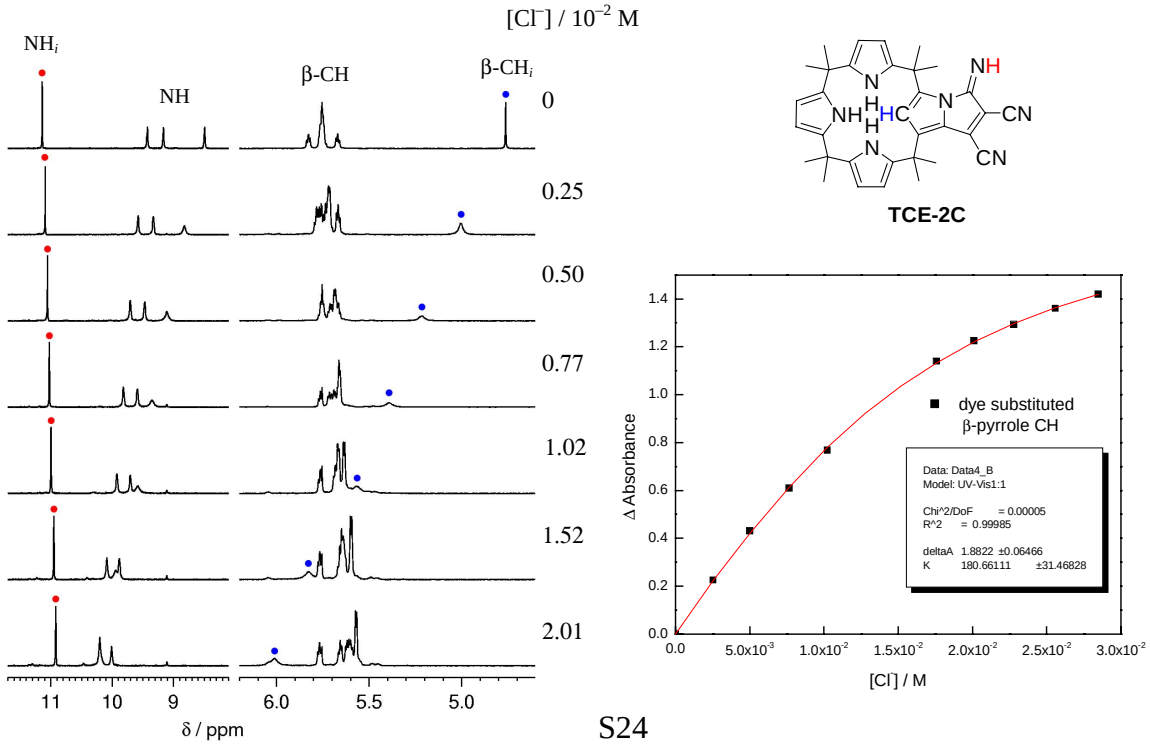

Figure S26. ^{1}H-NMR titration of **Azo-1** (1.0×10^{-2} M) with Cl^- in DMSO-d_6.

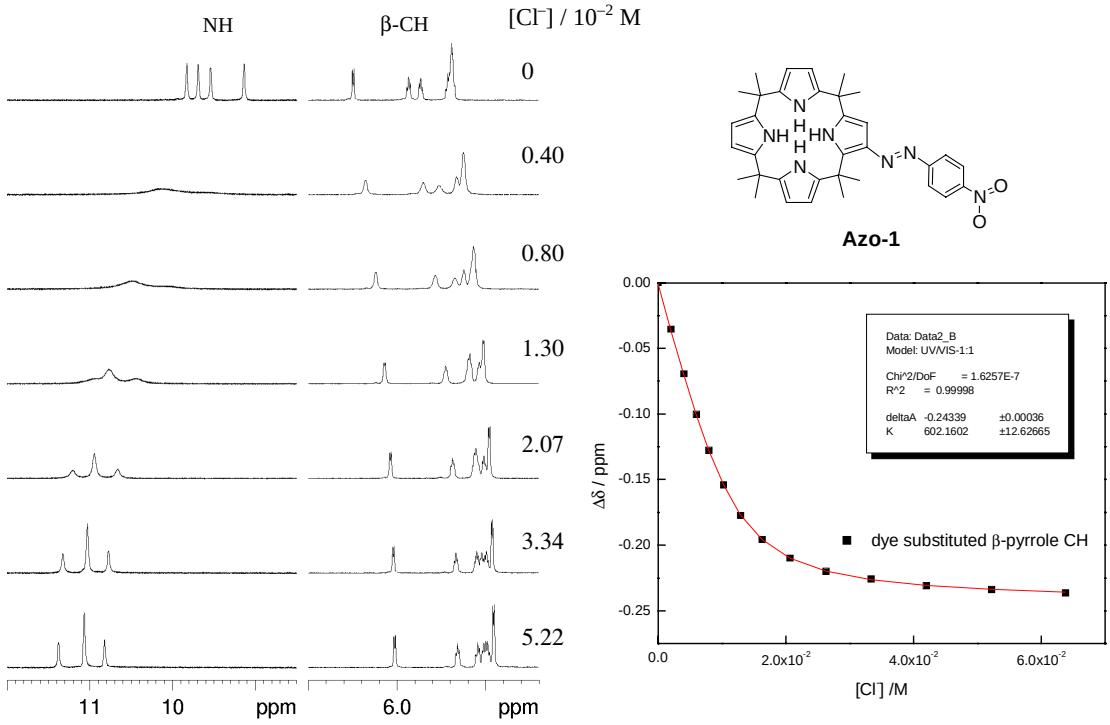

Figure S27. ^{1}H NMR titration of **Azo-2** (1.0×10^{-2} M) with Cl^- in DMSO-d_6. The inverted pyrrole ^{1}H resonances in **Azo-2** are labeled as follows: pyrrole NH_i ● and β-CH_i ●.

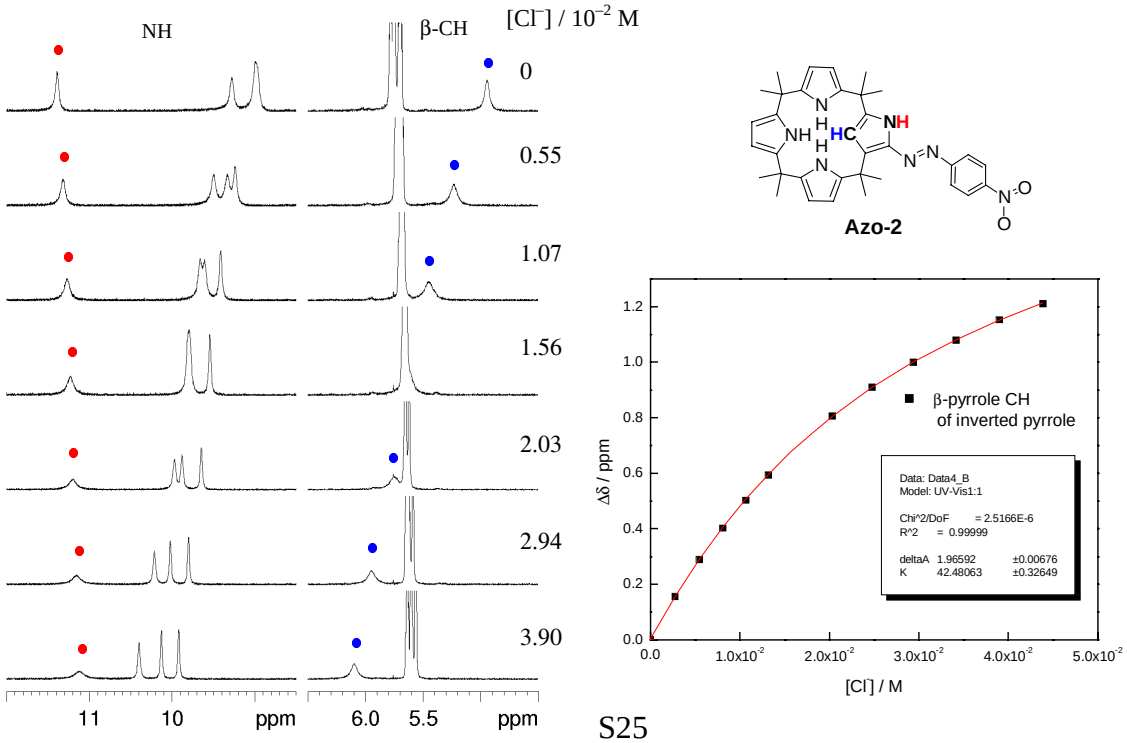

Figure S28. ^{1}H NMR titration of **1** (1.0x10^{-2} M) with F^{-} in DMSO-d_6.

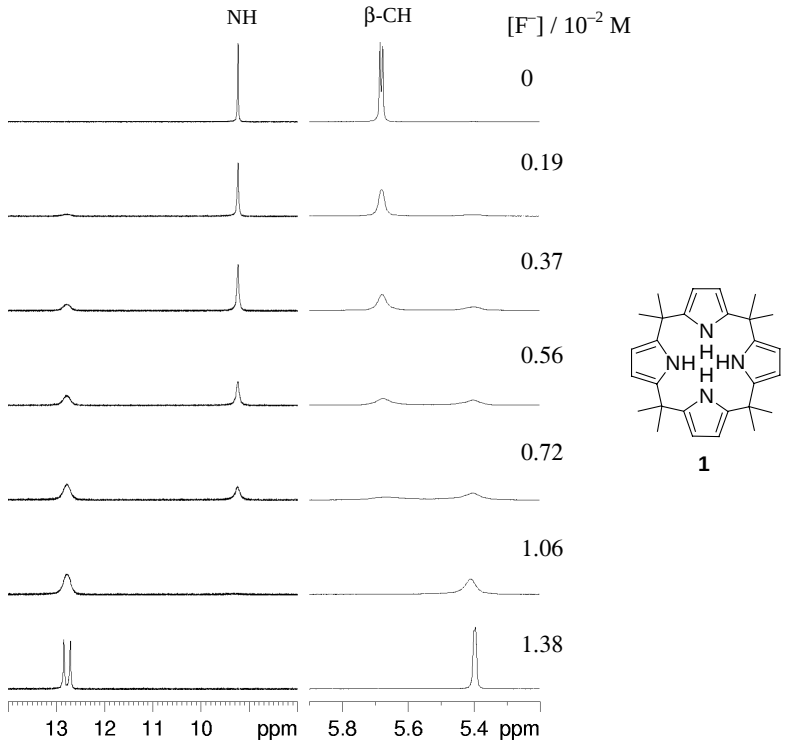

Figure S29. ^{1}H NMR titration of **2** (1.0x10^{-2} M) with F^{-} in DMSO-d_6. The inverted pyrrole ^{1}H resonances in **2** are labeled as follows: pyrrole NH$_i$ ●, α-CH$_i$ ●, and β-CH$_i$ ●.

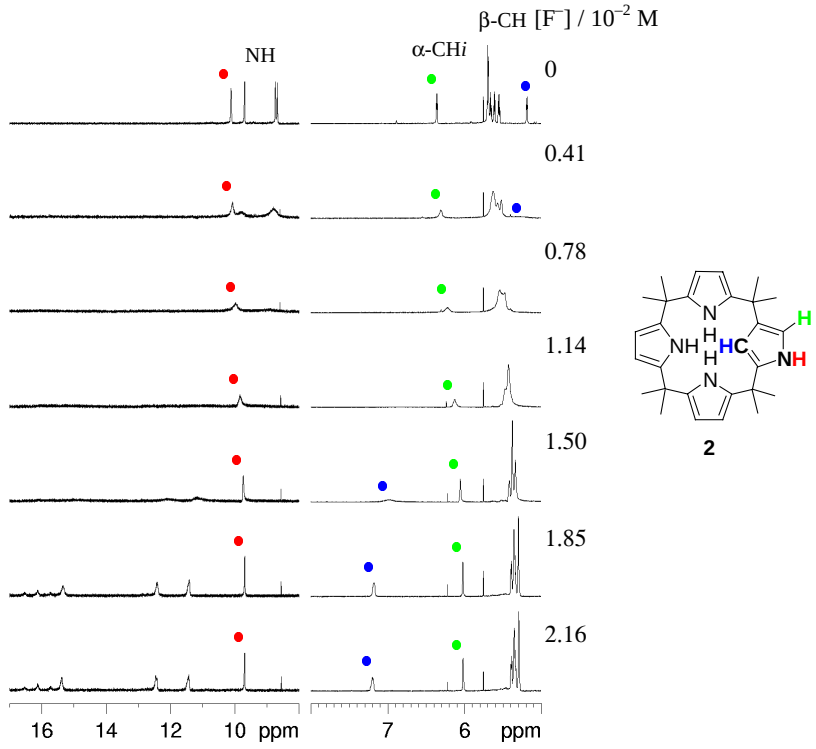

Figure S30. ^{1}H-NMR titration of **Azo-1** (1.0x10^{-2} M) with F^{-} in DMSO-d_6.

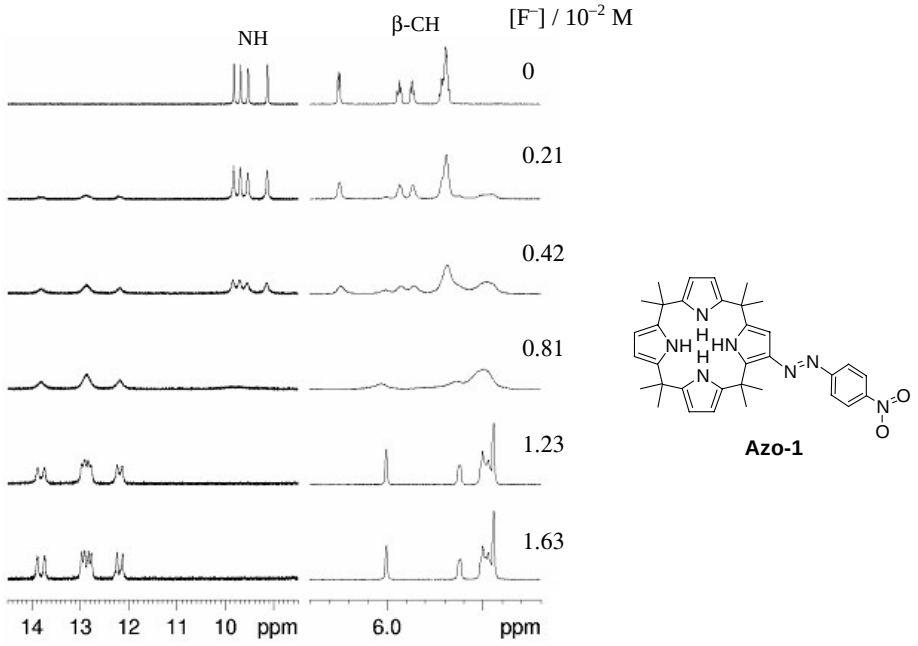

Figure S31. ^{1}H NMR titration of **Azo-2** (1.0x10^{-2} M) with F^{-} in DMSO-d_6. The inverted pyrrole ^{1}H resonances in **Azo-2** are labeled as follows: pyrrole NH$_i$ ● and β-CH$_i$ ●.

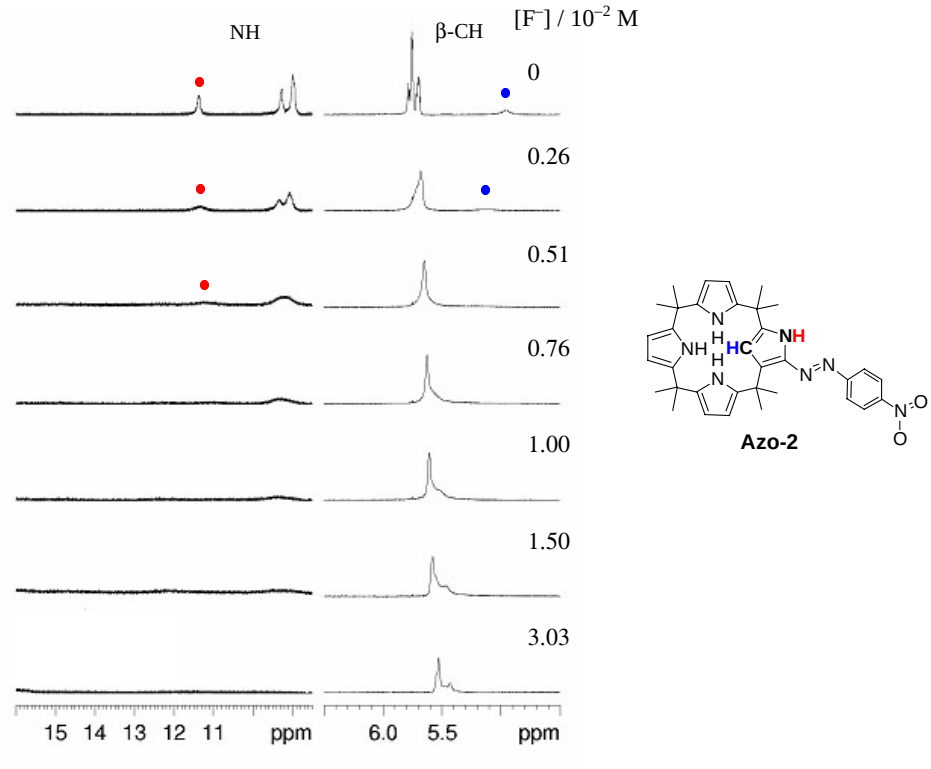

Density Functional Theory DFT Calculations.

Gaussian 03 (revision B.04)[9] was used for all the calculations presented. The calculations were carried out at the B3LYP[10] level of theory as it was priory reported in the literature for the same family of compounds.[11] For geometry optimizations the first guesses were fully optimized by PM3 semi-empirical Hamiltonian. Then, the models were re-optimized at B3LYP/6-31G* level of theory. Single Point Energies were calculated at B3LYP/6-31+G** level of theory. DFT-GIAO magnetic shielding were calculated at B3LYP/6-31G* level of theory in gas-phase.

• **Octamethylcalix[4]pyrrole-tetramethylammonium fluoride complex:**

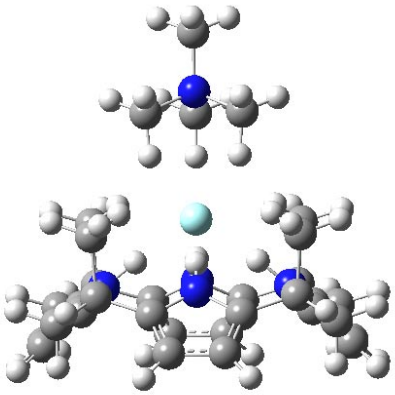

Energy=-1 621.944774 a.u.

Dipole Moment= 17.8862 debye

•***N*C-octamethylcalix[4]pyrrole-tetramethylammonium fluoride complex:**

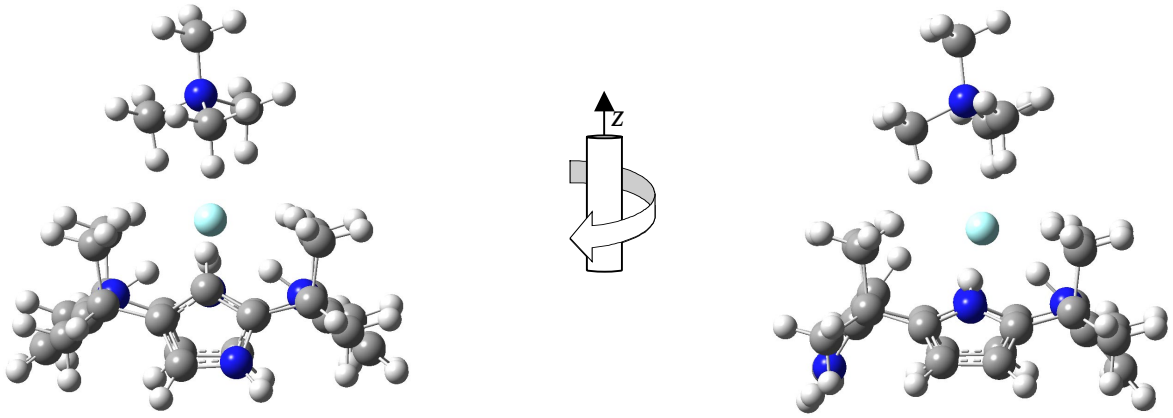

Energy=-1 621.935045 a.u.

Dipole Moment= 15.6695 debye

•Octamethylcalix[4]pyrrole-tetramethylammonium fluoride complex:

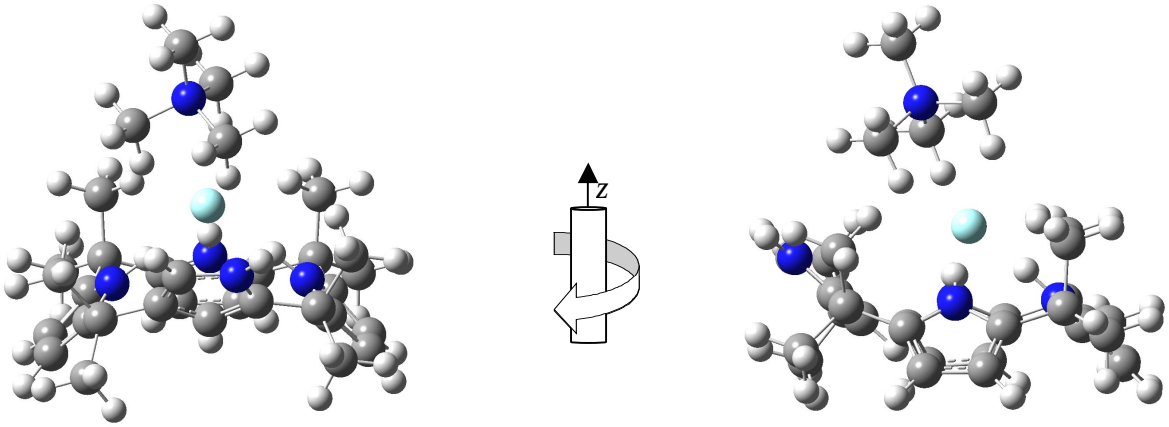

Energy=-1 621.88550210 a.u.

Dipole Moment= 16.9589 debye

•DFT-GIAO magnetic shielding calculation.

	B3LYP / 6-31G* GIAO Magnetic Shielding (ppm)			Experimental DMSO Titration		
H#	NC-OMCP	NC-OMCP •TMAF	²(ppm)	NC-OMCP	NC-OMCP •TBAF	²(ppm)
1	**25.510**	**21.045**	**4.465**	**9.698**	**12.400**	**2.702**
2	26.329	26.650	-0.322	5.688	5.350	-0.338
3	26.385	26.643	-0.258	5.656	5.350	-0.306
4	26.433	26.667	-0.234	5.549	5.350	-0.199
5	26.338	26.716	-0.377	5.688	5.350	-0.338
6	**25.864**	**22.193**	**3.671**	**8.678**	**11.440**	**2.762**
7	**25.810**	**22.549**	**3.261**	**8.736**	**11.440**	**2.704**
8	26.388	26.637	-0.249	5.608	5.350	-0.258
9	26.367	26.638	-0.271	5.688	5.350	-0.338
10	**25.506**	**25.528**	**-0.022**	**10.117**	**9.700**	**-0.417**
11	**25.909**	**26.139**	**-0.230**	**6.358**	**6.020**	**-0.338**
12	**27.108**	**24.213**	**2.895**	**5.183**	**7.190**	**2.007**

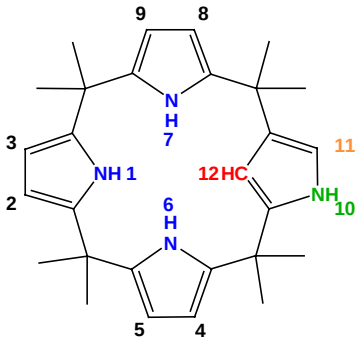

Anion Sensing of AZO1, AZO2, TCE1 and TCE2 embedded in polyurethane matrix:

Studies utilizing polyurethane matrices were performed using polymer films with incorporated sensors (**AZO1, AZO2, TCE1 and TCE2**), which were prepared by casting solutions containing sensors (aprox. 0.08% sensor in polyurethane, w/w) in Tecophilic™ SP-60D-16 (Figure S32) THF solution (6.5 % w/w) onto multi-well 10x8 (sub-microliter) size plate (Figure S33). The analyte was added (200 nL as aqueous solution (1-10mM) of the TBA (tetrabutylammonium) salts.

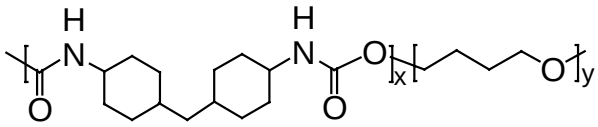

Figure S32. General structure of the polyurethane used in this study.[4]

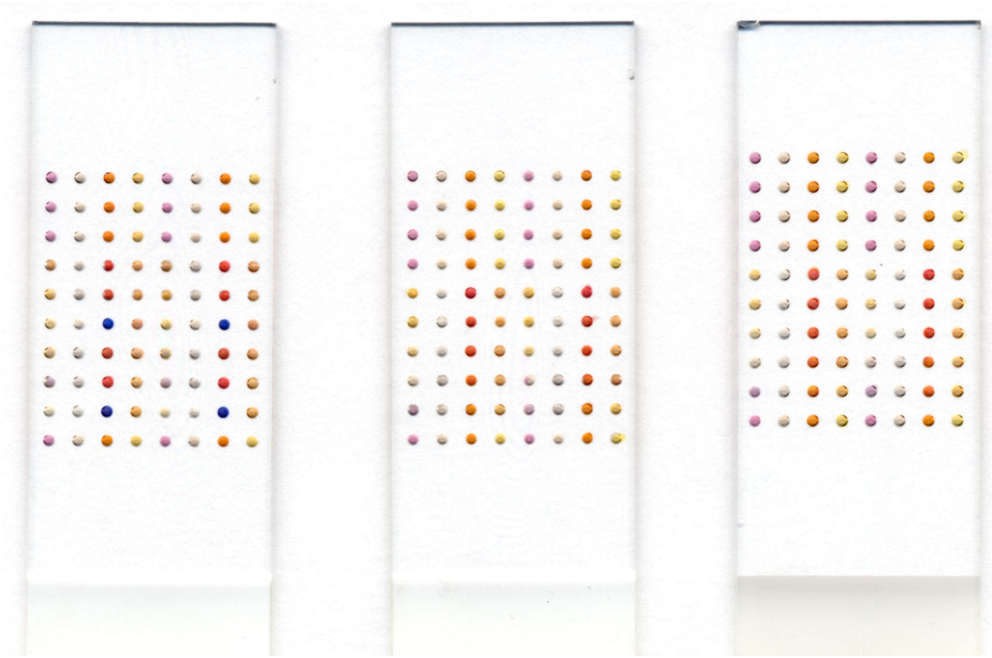

Figure S32. The scanner images (raw) of the sub-microliter assays. Top: multi-anion assay. Center: Acetate:phosphate competitive assay. Bottom: Acetate:chloride competitive assay. Note that each slide contains two essays.

References (Supporting Information).

(1) Connors, A. K. *Binding Constants: the Measurement of Molecular Complex Stability*; Wiley: New York, 1987.

(2) Gale, P. A.; Sessler, J. L.; Král, V.; Lynch, V. *J. Am. Chem. Soc.* **1996,** *118*, 5140-514.

(3) Depraetere, S.; Smet, M.; Dehaen, W. *Angew. Chem. Int. Ed.* **1999,** *38*, 3359-3361.

(4) Nishiyabu, R.; Anzenbacher, P., Jr. *J. Am. Chem. Soc.* **2005,** *127*, 8270-8271.

(5) Otwinowski, Z.; Minor, W. In DENZO-SMN., *Methods in Enzymology*; Macromolecular Crystallography 276; Carter, C. W., Jr., Sweets, R. M., Eds.; Academic Press: New York, 1997; part A, pp 307-326.

(6) Altomare, A.; Burla, M. C.; Camalli, M.; Cascarano, G. L.; Giacovazzo, C.; Guagliardi, A.; Moliterni, A. G. G.; Polidori, G.; Spagna, R. SIR97. A program for crystal structure solution. *J. Appl. Crystallogr.* **1999,** *32*, 115-119.

(7) Sheldrick, G. M. SHELXL97. *Program for the Refinement of Crystal Structures*; University of Gottingen, Germany, 1994.

(8) *International Tables for X-ray Crystallography*; Wilson, A. J. C., Eds.; Kluwer Academic Press: Boston, 1992; Vol. C, Tables 4.2.6.8 and 6.1.1.4.

(9) Frisch, M. J.; Trucks, G. W.; Schlegel, H. B.; Gill, P. M. W.; Johnson, B. G.; Robb, M. A.; Cheeseman, J. R.; Keith, T. A.; Peterson, G. A.; Montgomery, J. A.; Raghavachari, K.; Al-Laham, M. A.; Zakrzewski, V. G.; Ortiz, J. V.; Foresman, J. B.; Cioslowski, J.; Stefanov, B. B.; Nanayakkara, A.; Challacombe, M.; Peng, C. Y.; Ayala, P. Y.; Chen, W.; Wong, M. W.; Andres, J. L.; Replogle, E. S.; Gomperts, R.; Martin, R. L.; Fox, D. J.; Binkley, J. S.; Defrees, D. J.; Baker, J.; Stewart, J. P.; Head-Gordon, M.; Gonzalez, C.; Pople, J. A. *Gaussian 03 (Revision B.04)*; Gaussian, Inc.: Pittsburgh, PA, 2003.

(10) (a) Becke, A. D. *J. Chem. Phys.* **1993**, *98*, 5648. (b) Lee, C.; Yang,W.; Parr, R. G. *Phys. Re*V. *B* **1988**, *37*, 785. (c) Stevens, P. J.; Devlin, F. J.; Chablowski, C. F.; Frisch, M. J. *J. Phys. Chem.* **1994**, *98*, 11623.

(11) Wu, Y.; Wang, D.; Sessler, J. *J. Org. Chem.* **2001,** *66*, 3739-3746.